

# Weak magnetism and non-Fermi liquids near heavy-fermion critical points

T. Senthil

*Department of Physics, Massachusetts Institute of Technology, Cambridge MA 02139*

Matthias Vojta

*Institut für Theorie der Kondensierten Materie, Universität Karlsruhe, Postfach 6980, 76128 Karlsruhe, Germany*

Subir Sachdev

*Department of Physics, Yale University, P.O. Box 208120, New Haven CT 06520-8120*

(Dated: March 22, 2022)

This paper is concerned with the weak-moment magnetism in heavy-fermion materials and its relation to the non-Fermi liquid physics observed near the transition to the Fermi liquid. We explore the hypothesis that the primary fluctuations responsible for the non-Fermi liquid physics are those associated with the destruction of the large Fermi surface of the Fermi liquid. Magnetism is suggested to be a low-energy instability of the resulting small Fermi surface state. A concrete realization of this picture is provided by a fractionalized Fermi liquid state which has a small Fermi surface of conduction electrons, but also has other exotic excitations with interactions described by a gauge theory in its deconfined phase. Of particular interest is a three-dimensional fractionalized Fermi liquid with a spinon Fermi surface and a  $U(1)$  gauge structure. A direct second-order transition from this state to the conventional Fermi liquid is possible and involves a jump in the electron Fermi surface volume. The critical point displays non-Fermi liquid behavior. A magnetic phase may develop from a spin density wave instability of the spinon Fermi surface. This exotic magnetic metal may have a weak ordered moment although the local moments do not participate in the Fermi surface. Experimental signatures of this phase and implications for heavy-fermion systems are discussed.

## I. INTRODUCTION

The competition between the Kondo effect and inter-moment exchange determines the physics of a large class of materials which have localized magnetic moments coupled to a separate set of conduction electron [1]. When the Kondo effect dominates, the low-energy physics is well described by Fermi liquid theory (albeit with heavily renormalized quasiparticle masses). In contrast when the inter-moment exchange dominates, ordered magnetism typically results.

A remarkable experimental property of such magnetic states is that the magnetism is often very weak – the ordered moment per site is much smaller than the microscopic local moment that actually occupies each site. The traditional explanation of this feature is that the magnetism arises out of imperfectly Kondo-screened local moments. In other words, the magnetism is to be viewed as a spin density wave that develops out of the parent heavy Fermi liquid state. We will henceforth denote such a state as SDW. Clearly a SDW state may be a small moment magnet.

A different kind of magnetic metallic state is also possible in heavy-fermion materials where the moments order at relatively large energy scales, and simply do not participate in the Fermi surface of the metal. In such a situation, the saturation moment in the ordered state would naively be large, *i.e.*, of order the atomic moment.

Often the distinction between these two kinds of magnetic states can be made sharply: the two Fermi surfaces in the two states may have different topologies (albeit,

the same volume modulo the volume of the Brillouin zone of the ordered state), so that they cannot be smoothly connected to one another.

In recent years, a number of experiments have unearthed some fascinating phenomena near the zero temperature ( $T$ ) quantum transition between the heavy-fermion liquid and the magnetic metal. In particular, many experiments do not fit easily [2, 3, 4, 5] into a description in terms of an effective Gaussian theory for the spin density wave fluctuations, renormalized self-consistently by quartic interactions [6, 7, 8, 9, 10]. This theory makes certain predictions on deviations from Fermi liquid behavior as the heavy Fermi liquid state approaches magnetic ordering induced by the condensation of the spin density wave mode; those predictions are, however, in disagreement with experimental findings. This conflict raises the possibility that the magnetic state being accessed is not in the first category discussed above: a SDW emerging from a heavy Fermi liquid. Rather, it may be the second kind of magnetic metal where the local moments do not participate at all in the Fermi surface. In other words, the experiments suggest that the Kondo effect (crucial in forming the Fermi liquid state) is itself suppressed on approaching the magnetic state.

This proposal clearly raises several serious puzzles. How do we correctly describe the non-Fermi liquid physics near the transition? If this non-Fermi liquid behavior is accompanied by the suppression of the Kondo effect, how do we reconcile it with the weak moments found in the magnetic state? The traditional explanation for the weak magnetism is apparently in conflict

with the picture that the Kondo effect and the resultant heavy Fermi liquid state are destroyed on approaching the magnetic state. In other words, the naive expectation of a large saturation moment in a magnetic metal where the local moments do not participate in the Fermi surface must be revisited.

The weakness of the ordered moment in the magnetic state may be reconciled with the apparent suppression of the Kondo effect if we assume that there are strong quantum fluctuations of the spins that reduce their moment. Such strong quantum effects may appear to be unusual in three-dimensional systems, but may be facilitated by the coupling to the conduction electrons (even if there is no actual Kondo screening). In this paper we study specific states where such quantum fluctuations have significantly reduced the ordered moment (or even caused it to vanish), and the evolution of such states to the heavy Fermi liquid.

We begin with several general pertinent observations. First, consider the heavy Fermi liquid state. This Fermi liquid behavior is accompanied by a Fermi surface which, remarkably, satisfies Luttinger's theorem only if the local moments are included as part of the electron count. (Such a Fermi surface is often referred to as the “large Fermi surface”, and we will henceforth refer to such a phase as FL). The absorption of the local moments into the Fermi volume is the lattice manifestation of the Kondo screening of the moments. We take as our starting point the assumption that the Kondo effect becomes suppressed on approaching the magnetic state. What then happens to the large Fermi surface?

In thinking about the resulting state theoretically, it is important to realize that once magnetic order sets in, there is no sharp distinction between a large Fermi volume which includes the local moments, and a Fermi volume that excludes the local moments – the latter is often loosely referred to as “small”. This is because the Fermi volumes can only be defined modulo the volume of the Brillouin zone, and the onset of magnetic order at least doubles the unit cell and hence at least halves the Brillouin zone volume. (There can, however, be a distinction between the Fermi surfaces topologies in the two situations.)

In this paper we will take the point of view that the primary transition involves the destruction of the large Fermi surface, and that the resulting small Fermi surface state has a distinct physical meaning even in the absence of magnetic order. The magnetic order will be viewed as a low-energy instability of the resulting state in which the local moments are not to be included in the Fermi volume.

Evidence in support of this point of view exists. In the experiments the non-Fermi liquid behavior extends to temperatures well above the Neel ordering temperature even far away from the critical point. This suggests that the fluctuations responsible for the non-Fermi liquid behavior have very little to do with the fluctuations of the magnetic order parameter. Some further support

is provided by the results of inelastic neutron scattering experiments that apparently see critical behavior at a range of wave-vectors including (but not restricted to) the one associated with magnetic ordering in the magnetic metal [5]. Finally, there even exist materials in which the non-Fermi liquid features persist into the magnetically ordered side – this is difficult to understand if the non-Fermi liquid physics is attributed to critical fluctuations of the magnetic order parameter.

Conceptually, as we asserted above, it pays to allow for the possibility of a non-magnetic state in which the suppression of the Kondo effect removes the local moments from the Fermi volume, resulting in a “small Fermi surface”, even though such a state may not actually be a ground state in the system of interest. In our previous work [11] we argued that such states do exist as ground states of Kondo lattice models in regular  $d$ -dimensional lattices, and that the violation of Luttinger's theorem in such a state was intimately linked to the presence of neutral  $S = 1/2$  and  $S = 0$  excitations induced by topological order (see also Appendix A): we dubbed such ground states FL\*.

Clearly, it is worthwhile to explore metallic magnetic states that develop out of such FL\* states (just as the usual SDW state develops out of the Fermi liquid). Such states, which we will denote SDW\*, represent a third class of metallic magnetic states distinct from both the conventional SDW and the conventional local-moment metal described above. As we will see, in such magnetic states the local moments do not participate in the Fermi surface. Nevertheless they may have a weak ordered moment. Thus these states offer an opportunity for resolution of the puzzles mentioned above. The properties and the evolution of such states, and their parent FL\* states, to the Fermi liquid will be the subject of this paper. The SDW\* states inherit neutral spin  $S = 1/2$  spinon excitations and  $S = 0$  “gauge” excitations from the FL\* states, which will be described more precisely below; these excitations coexist with the magnetism and the metallic behavior. The experimental distinction between the SDW and SDW\* states is however subtle, and will also be described in this paper. (The FL and FL\* states can be easily distinguished by the volumes of the Fermi surfaces, but this distinction does not extend to the SDW and SDW\* states.)

We emphasize that a wide variety of heavy-fermion materials display non-Fermi liquid physics in the vicinity of the onset of magnetism that is, to a considerable extent, universal. However, the detailed behavior at very low temperature appears to vary across different systems. In particular, in some materials a direct transition to the magnetic state at very low temperature does not occur (due for instance to intervention of a superconducting state). In other materials, such a direct transition does seem to occur at currently accessible temperatures. In view of this, we will not attempt to predict the detailed phase diagram at ultra-low temperatures. We focus instead on understanding the universal non-Fermi liquid

physics not too close to the transition and its relation to the magnetic state.

### A. Summary of results

Our analysis is based upon non-magnetic translation-invariant states that have a small Fermi surface (FL\*), and the related transitions to the heavy Fermi liquid (FL). As we showed previously [11], the FL\* state has a Fermi surface of long-lived electron-like quasiparticles whose volume does not count the local moments. The local moments are instead in a state adiabatically connected to a spin-liquid state with emergent gauge excitations. Such spin liquids can be classified by the gauge group determining the quantum numbers carried by the neutral  $S = 1/2$  spinon excitations and the gauge excitations, and previous work [12, 13] has shown that the most prominent examples are  $Z_2$  and U(1) spin liquids. The  $Z_2$  spin liquids are stable in all spatial dimensions  $d \geq 2$ , while the U(1) spin liquids exist only in  $d \geq 3$  (the latter correspond to the existence of a Coulomb phase in a compact U(1) gauge theory in  $d \geq 3$ , as discussed in Ref. 14). Correspondingly, we also have the metallic  $Z_2$  FL\* and U(1) FL\* states. Our previous work [11] considered primarily the  $Z_2$  FL\* state, whereas here we focus on the U(1) FL\* state.

As we have already discussed, these non-magnetic states may lead to magnetic order at low energies, or in proximate states in a generalized phase diagram. In this manner the FL state leads to the SDW state, while the FL\* states lead to the  $Z_2$  SDW\* and the U(1) SDW\* states. The relation between the metallic SDW and SDW\* states has a parallel to that between the insulating Néel state and the AF\* state of Refs. 13, 15.

We will also discuss the evolution from the U(1) SDW\* state to the conventional Fermi liquid. As explained earlier, the underlying transition is that between FL and FL\* states which controls the nature of the Fermi surface. In Ref. 11, we argued that the spinon pairing in the  $Z_2$  FL\* state implied that there must be a superconducting state in between the FL and  $Z_2$  FL\* states. There is no such pairing in the U(1) FL\* state, and hence there is the possibility of a direct transition between the FL and U(1) FL\* states: this transition and the nature of the states flanking it are the foci of our paper. Note that the volume of the Fermi surface *jumps* at this transition. Nevertheless the transition may be second order. This is made possible by the vanishing of the quasiparticle residue on an entire portion of the Fermi surface (a “hot” Fermi surface) on approaching the transition from the FL side. Non-Fermi liquid physics is clearly to be expected at such a second order Fermi-volume changing transition. We reiterate that the U(1) FL\* state is only believed to exist in  $d > 2$ .

We study the FL and U(1) FL\* states by the “slave” boson method, introduced in the context of the single-moment Kondo problem [16]. In this method, the con-

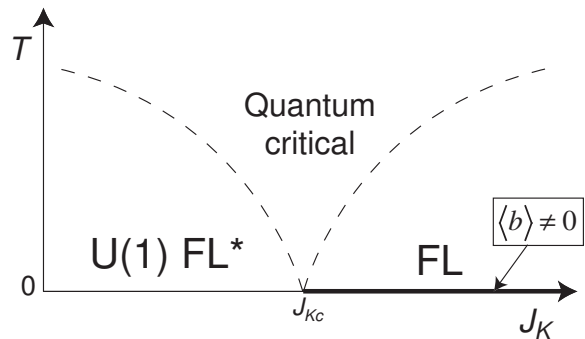


FIG. 1: Crossover phase diagram for the vicinity of the  $d = 3$  quantum transition involving breakdown of Kondo screening.  $J_K$  is the Kondo exchange in the Hamiltonian introduced in Section III. The only true phase transition above is that at the  $T = 0$  quantum critical point at  $J_K = J_{Kc}$  between the FL and FL\* phases. The “slave” boson  $b$  measures the mixing between the local moments and the conduction electrons and is also described in Section III. The crossovers are similar to those of a dilute Bose gas as a function of chemical potential and temperature, as discussed in Refs. 19, 20—the horizontal axis is a measure of the boson chemical potential  $\mu_b$ . The boson is coupled to a compact U(1) gauge field; at  $T = 0$  this gauge field is in the Higgs/confining phase in the FL state, and in the deconfining/Coulomb phase in the FL\* state. There is no phase transition at  $T > 0$  between a phase with  $\langle b \rangle \neq 0$  and a phase with  $\langle b \rangle = 0$  because such a transition is absent in a theory with a compact U(1) gauge field in  $d = 3$  [21] (the mean-field theories of Sections. III and IV C do show such transitions, but these will turn into crossovers upon including gauge fluctuations). The compactness of the gauge field therefore plays a role in the crossovers in the “renormalized classical” regime above the FL state (this has not been worked out in any detail here). However, the compactness is not expected to be crucial in the quantum-critical regime. The crossover line displayed between the FL and quantum critical regimes can be associated with the “coherence” temperature of the heavy Fermi liquid. At low  $T$ , as discussed in the text, there are likely to be additional phases associated with magnetic order (the SDW and SDW\* phases), and these are not shown above but are shown in Fig. 2; they also appear in the mean-field phase diagram in Fig. 4.

densation of the slave boson marks the onset of Kondo coherence that characterizes the FL phase. In contrast the slave boson is not condensed in the FL\* phase. Fluctuations about this mean-field description lead to the critical theory of the transition involving a propagating boson coupled to a compact U(1) gauge field, in the presence of damping from fermionic excitations.

We note that earlier studies [17, 18] of single-impurity problems found a temperature-induced mean-field transition between a state in which the slave boson is condensed (and hence the local moment is Kondo screened) and a state in which the boson has no condensate: however, it was correctly argued that this transition is an artifact of the mean-field theory, and no sharp transition exists in the single-moment Kondo problem at  $T > 0$ . If we now naively generalize this single-impurity model

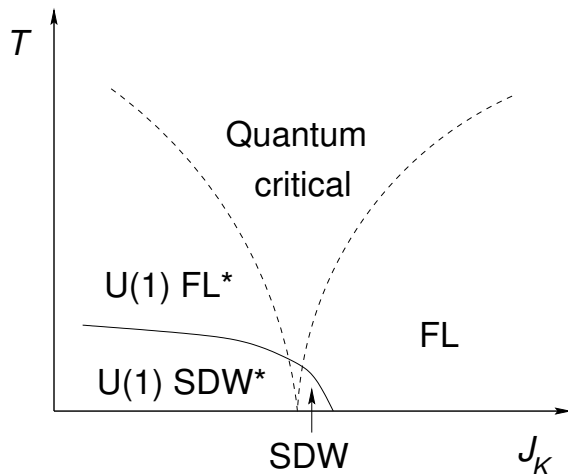


FIG. 2: Expected phase diagram and crossovers for the evolution from the U(1) SDW\* phase to the conventional FL. Two different transitions are *generically* possible at zero temperature: Upon moving from the SDW\* towards the Fermi liquid, the fractionalization is lost first followed by the disappearance of magnetic order. Nevertheless the higher temperature behavior in the region marked ‘quantum critical’ is non-fermi liquid like, and controlled by the Fermi volume changing transition from FL to FL\*. This may be loosely associated to the breakdown of Kondo screening.

to the lattice, we will find that the  $T = 0$  ground state always has Kondo screening. It is only upon including frustrating inter-moment exchange interactions – equivalent to having “dispersing” spinons – that it is possible to breakdown Kondo screening and reach a state in which the slave boson is not condensed. This transition is not an artifact of mean-field theory, we show here that it remains sharply defined in  $d = 3$ .

Our analysis of the above  $d = 3$  U(1) gauge theory leads to the schematic crossover phase diagram as a function of the Kondo exchange  $J_K$  and  $T$  shown in Fig 1.

The crossover phase diagram in Fig. 1 is similar to that of a dilute Bose gas as a function of chemical potential and temperature [19, 20]. Here the bosons are coupled to a U(1) gauge field, and this is important for many of the critical properties to be described in the body of the paper. Notably, in Fig. 1 the density of bosons is *not* fixed, and varies as a function of  $T$ ,  $J_K$  and other couplings in the Hamiltonian. Indeed, the contours of constant boson density have a complicated structure, which are similar to those in Ref. 20. This variation in the boson density is a crucial distinction from earlier analyses [22, 23] of boson models coupled to damped U(1) gauge fields: in these earlier works, the boson density was fixed at a  $T$ -independent value. As we will see, allowing the boson density to vary changes the critical properties, and has significant consequences for the structure of the crossover phase diagram and for the  $T$  dependence of observables.

We will show that non-Fermi liquid physics obtains in the quantum critical region of this transition. Furthermore, we argue that fluctuation effects may lead to a spin

density wave developing out of the spinon Fermi surface of the U(1) FL\* phase, thereby obtaining the U(1) SDW\* phase. The expected phase diagram and crossovers for the evolution from the U(1) SDW\* phase to the FL phase is shown in Fig. 2. We examine few different kinds of such U(1) SDW\* phases depending on the details of the spinon Fermi surface. We also describe a number of specific experimental signatures of the U(1) SDW\* phase which may help to distinguish it from more conventional magnetic metals.

## B. Relation to earlier work

We have already mentioned a number of precursors to our ideas in our discussion so far. Here, we complete this by noting some other related developments in the literature.

Early on, Andrei and Coleman [24] and Kagan *et al.* [25] discussed the possibility of the decoupling of local moments and conduction electrons in Kondo lattice models. Andrei and Coleman had the local moments in a spin-liquid state which is unstable to U(1) gauge fluctuations, and did not notice violation of Luttinger’s theorem. The possibility of small electronic Fermi surfaces was noted by Kagan *et al.*, but no connection was made to the requirement this imposes on emergent gauge excitations [11].

More recently, Burdin *et al.* described many aspects of the physics we are interested in a dynamical mean-field theory of a random Kondo lattice [26]. In this work, they obtained a state in which local moments formed a spin liquid and stayed essentially decoupled from the conduction electrons. They emphasized that the transition between such a state (which is the analog of our FL\* states) and a conventional heavy Fermi liquid (the FL state) should be understood as a Fermi volume changing transition. However questions of emergent gauge structure were not addressed by them.

Demler *et al.* [27] discussed fractionalized phases of Kondo lattice models. However, they did not consider any states with long-lived electron-like quasiparticles, as are present in the FL\* phase.

Recently Essler and Tsvelik [28] discussed the fate of one-dimensional Mott insulator under a particular long-range inter-chain hopping. At intermediate temperatures, they obtain a state with a small Fermi surface, in that the Fermi surface volume does not count the local moments [29]. However, their construction does not lead to a state with emergent gauge excitations in higher dimensions, and as they conclude, their state is unstable to magnetic order at low temperatures. We believe this low- $T$  state is an ordinary SDW state, and any realizations of small Fermi surfaces at intermediate temperatures are remnants of one-dimensional physics. In contrast, all our constructions are genuinely higher-dimensional, and only work for  $d \geq 2$ .

The physics of the destruction of the large Fermi sur-

face by the vanishing of Kondo screening has been addressed in interesting recent works [30, 31, 32] using an “extended dynamical mean-field theory”. We have argued in our discussion above that vanishing of Kondo screening is conceptually quite a different transition from the onset of magnetic order; consistent with this expectation, Sun and Kotliar [31] found two distinct points associated with these transitions. It is our contention that the critical theory of the FL to U(1) FL\* transition (discussed in the present paper) is the  $d = 3$  realization of the large-dimensional critical point with vanishing Kondo screening found by Sun and Kotliar.

### C. Outline

The rest of the paper is organized as follows: In Section II, we briefly review the properties of various fractionalized Fermi liquids (FL\*). A specific U(1) FL\* state where the spinons form a Fermi surface is considered. In Section III, we construct a mean-field description of this state and its transition to the heavy Fermi liquid. This transition involves a jump in the Fermi surface volume but is nevertheless shown to be second order within the mean-field theory. This is made possible by the vanishing of the quasiparticle residue  $Z$  on an entire Fermi surface (a “hot” Fermi surface) as one moves from the heavy Fermi liquid to the fractionalized Fermi liquid. Fluctuations about this mean-field description are then considered. In Section IV, we first consider fluctuation effects on the phases – in particular the FL\* phase. We argue that the specific heat coefficient  $\gamma$  diverges logarithmically once the leading-order fluctuations are included. Furthermore, fluctuations also make possible a spin density wave instability of the spinon Fermi surface, leading to a U(1) SDW\* state. To illustrate possible phases, we will discuss an improved mean-field theory which includes the SDW order parameter, and present phase diagrams showing the influence of temperature and magnetic field. We then examine fluctuation effects at the critical point of the transition between FL\* and FL in Section V. We argue that the logarithmic divergence of the specific heat coefficient persists in the quantum critical region, and also that non-Fermi liquid transport obtains there. In Section VI, we discuss the properties of the U(1) SDW\* phase in greater detail with particular attention to its identification in experiments. A discussion of the implications for various experiments in Sec. VII will conclude the paper.

## II. FRACTIONALIZED FERMIL LIQUIDS

The existence of non-magnetic translation invariant “small Fermi surface” states was shown in a recent article by us [11] with a focus on two-dimensional Kondo lattices. Such states were obtained when the local-moment system settles into a fractionalized spin liquid (rather

than a magnetically ordered state) due to inter-moment interactions. A weak Kondo coupling to conduction electrons does not disrupt the structure of the spin liquid but leaves a sharp Fermi surface of quasiparticles whose volume counts the conduction electron density alone (a small Fermi surface). Thus these states have fractionalized excitations that coexist with conventional Fermi-liquid-like quasiparticle excitations. We dubbed these states FL\* (to distinguish them from the conventional Fermi liquid FL). We also pointed out an intimate connection between the disappearance of the large Fermi surface and fractionalization, and this is discussed further in Appendix A.

The FL\* phase can be further classified by the nature of the spin liquid formed by the local moments. Recent years have seen considerable progress in our understanding of fractionalized spin liquids. An important feature of spin liquid states in  $d \geq 2$  is that they possess emergent gauge structure. Put simply, this means that the distinct excitations in such phases interact with each other through long ranged interactions which can be mathematically encapsulated as gauge interactions. In other words, the effective field theory of the state is a gauge theory in its deconfined phase. The two natural possibilities are that the emergent gauge group is either  $Z_2$  or U(1). The former is allowed in any dimension  $d \geq 2$  while the latter is only allowed in  $d = 3$  (or higher).

The  $Z_2$  states have been discussed at length in the literature and in the present context in our earlier work [11]. In contrast, the U(1) states have not been discussed much, though their possible occurrence (in  $d = 3$ ) and their universal properties have been appreciated by many workers in the field. We therefore provide a quick discussion: The distinct excitations in the  $d = 3$  U(1) spin liquid phases are neutral spin-1/2 spinons, a gapless (emergent) gauge photon, and a gapped point defect (the “monopole”). The spinons are minimally coupled to the photon and hence interact through emergent long ranged interactions. For simple microscopic models that realize such phases, see Ref. 14, 33. A crucial distinction between the  $Z_2$  spin liquids is that the spinons in this phase are *not* generically paired, *i.e.*, the spinon number is conserved [34].

Several classes of spin liquids are theoretically possible with the same gauge structure. These may be characterized by the statistics of the spinons, their band structure, etc. For the rest of this paper, we will focus on a particular three-dimensional U(1) spin liquid state with fermionic spinons that form a Fermi surface. A specific toy model which displays this phase is presented in Appendix B.

As with the  $Z_2$  spin liquids discussed in Ref. 11, the gauge structure in the U(1) spin liquid state is also stable to a weak Kondo coupling to conduction electrons [35]. The resulting U(1) FL\* state consists of a spinon Fermi surface coexisting with a separate Fermi surface of conduction electrons. There will also be gapless photon and gapped monopole excitations. The physical electron

Fermi surface (as measured by de-Haas van Alphen experiments for instance) will have a small volume that is determined by the conduction electrons alone.

In our previous work, we pointed out that the transition from a  $Z_2$  FL\* phase to the heavy FL will generically be preempted by superconductivity. This is due to the pairing of spinons in the  $Z_2$  phase. In contrast, we expect that due to conservation of spinon number a direct transition between the U(1) FL\* and heavy FL phases should be possible.

### III. MEAN-FIELD THEORY

A simple mean-field theory allows a description both of a U(1) FL\* phase and its transition to the heavy FL. Consider a three-dimensional Kondo-Heisenberg model, for concreteness on a cubic lattice:

$$H = \sum_k \epsilon_k c_{k\alpha}^\dagger c_{k\alpha} + \frac{J_K}{2} \sum_r \vec{S}_r \cdot c_{r\alpha}^\dagger \vec{\sigma}_{\alpha\alpha'} c_{r\alpha'} + J_H \sum_{\langle rr' \rangle} \vec{S}_r \cdot \vec{S}_{r'}. \quad (1)$$

Here  $c_{k\alpha}$  represent the conduction electrons and  $\vec{S}_r$  the spin-1/2 local moments on the sites of a cubic lattice, summation over repeated spin indices  $\alpha$  is implicit. We use a fermionic “slave-particle” representation of the local moments:

$$\vec{S}_r = \frac{1}{2} f_{r\alpha}^\dagger \vec{\sigma}_{\alpha\alpha'} f_{r\alpha'} \quad (2)$$

where  $f_{r\alpha}$  describes a spinful fermion destruction operator at site  $r$ .

Proceeding as usual, we consider a decoupling of both the Kondo and Heisenberg exchange using two auxiliary fields in the particle-hole channel. Treating the fluctuations of these auxiliary fields by a saddle point approximation (formally justified for a large- $N$  SU( $N$ ) generalization), we obtain the mean-field Hamiltonian

$$H_{\text{mf}} = \sum_k \epsilon_k c_{k\alpha}^\dagger c_{k\alpha} - \chi_0 \sum_{\langle rr' \rangle} (f_{r\alpha}^\dagger f_{r'\alpha} + \text{h.c.}) + \mu_f \sum_r f_{r\alpha}^\dagger f_{r\alpha} - b_0 \sum_k (c_{k\alpha}^\dagger f_{k\alpha} + \text{h.c.}) \quad (3)$$

where we assumed  $\chi_0$  and  $b$  to be real, and have dropped additional constants to  $H$ . The mean-field parameters  $b_0, \chi_0, \mu_f$  are determined by the conditions

$$1 = \langle f_{r\alpha}^\dagger f_{r\alpha} \rangle, \quad (4)$$

$$2b_0 = J_K \langle c_{r\alpha}^\dagger f_{r\alpha} \rangle, \quad (5)$$

$$2\chi_0 = J_H \langle f_{r\alpha}^\dagger f_{r'\alpha} \rangle. \quad (6)$$

In the last equation  $r, r'$  are nearest neighbors.

There are two qualitatively different zero-temperature phases. First, there is the usual Fermi liquid (FL) phase

when  $b_0, \chi_0, \mu_f$  are all non-zero. (Note that  $b_0 \neq 0$  implies that  $\chi_0 \neq 0$ ). This phase is readily seen to have a large Fermi surface as expected. Second, there is a phase (FL\*) where the Kondo hybridization  $b_0 = 0$  but  $\chi_0 \neq 0$ . (In this phase  $\mu_f = 0$ .) This mean-field state represents a situation where the conduction electrons are decoupled from the local moments and form a *small* Fermi surface. The local-moment system is described as a spin fluid with a Fermi surface of neutral spinons. We expect that  $\chi_0 \sim J_H$ .

The transition between these two different states can also be examined within the mean-field theory. Interestingly, the transition is second order (despite the jump in Fermi volume) and is described by  $b_0 \rightarrow 0$  on approaching it from the Fermi liquid side. How can a second order transition be associated with a jump in the volume of the electron Fermi surface? This can be understood by examining the Fermi surfaces closely in this mean-field theory.

The mean-field Hamiltonian is diagonalized by the transformation

$$\begin{aligned} c_{k\alpha} &= u_k \gamma_{k\alpha+} + v_k \gamma_{k\alpha-}, \\ f_{k\alpha} &= v_k \gamma_{k\alpha+} - u_k \gamma_{k\alpha-}. \end{aligned} \quad (7)$$

Here  $\gamma_{k\alpha\pm}$  are new fermionic operators in terms of which the Hamiltonian takes the form

$$H_{\text{mf}} = \sum_{k\alpha} E_{k\pm} \gamma_{k\alpha+}^\dagger \gamma_{k\alpha+} + E_{k-} \gamma_{k\alpha-}^\dagger \gamma_{k\alpha-}, \quad (8)$$

with

$$E_{k\pm} = \frac{\epsilon_k + \epsilon_{kf}}{2} \pm \sqrt{\left(\frac{\epsilon_k - \epsilon_{kf}}{2}\right)^2 + b_0^2}. \quad (9)$$

Here  $\epsilon_{kf} = \mu_f - \chi_0 \sum_{a=1,2,3} \cos(k_a)$ . The  $u_k, v_k$  introduced above are determined by

$$u_k = -\frac{b_0 v_k}{E_{k+} - \epsilon_k}, \quad u_k^2 + v_k^2 = 1. \quad (10)$$

Consider first the FL\* phase where  $b_0 = 0 = \mu_f$ , but  $\chi_0 \neq 0$ . The electron Fermi surface is determined by the conduction electron dispersion  $\epsilon_k$  and is small. The spinon Fermi surface encloses one spinon per site and has volume half that of the Brillouin zone. For concreteness, we will consider the situation where the electron Fermi surface does not intersect the spinon Fermi surface. We will also assume that the conduction electron filling is less than half.

Now consider the FL phase near the transition (small  $b_0$ ). In this case, there are two bands corresponding to  $E_{k\pm}$ : one derives from the  $c$ -electrons (with weak  $f$  character) while the other derives from the  $f$ -particles (with weak  $c$ -character). We will call the former the  $c$ -band and the latter the  $f$ -band. For small  $b_0$ , both bands intersect the Fermi energy so that the Fermi surface consists of two sheets (see Fig. 3). The total volume is large, *i.e.*,

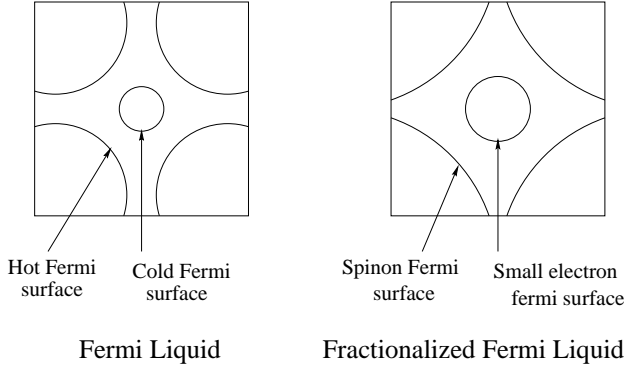


FIG. 3: Fermi surface evolution from FL to FL\*: close to the transition, the FL phase features two Fermi surface sheets (the cold  $c$  and the hot  $f$  sheet, see text). Upon approaching the transition, the quasiparticle residue  $Z$  on the hot  $f$  sheet vanishes. On the FL\* side, the  $f$  sheet becomes the spinon Fermi surface, whereas the  $c$  sheet is simply the small conduction electron Fermi surface.

includes both local moments and conduction electrons. Upon moving toward the transition to FL\* ( $b_0$  decreasing to zero), the  $c$ -Fermi surface expands in size to match onto the small Fermi surface of FL\*. On the other hand, the  $f$ -Fermi surface shrinks to match onto the *spinon* Fermi surface of FL\*.

Upon increasing  $b_0$  in the FL state and depending on the band structure, another transition is possible, where the  $c$  band becomes completely empty. Then, the Fermi surface topology changes from two sheets to a single sheet – such a transition between two conventional Fermi liquids is known as Lifshitz transition and will not be further considered here.

The quasiparticle weight  $Z$  close to the FL–FL\* transition is readily calculated in the present mean-field theory. For the electron Green’s function we find

$$\mathcal{G}(k, i\omega_\nu) = \frac{u_k^2}{i\omega_\nu - E_{k+}} + \frac{v_k^2}{i\omega_\nu - E_{k-}}. \quad (11)$$

Therefore at the Fermi surface of the  $c$ -band (which has dispersion  $E_{k+}$ , the quasiparticle residue  $Z = u_k^2$ . At this Fermi surface,  $E_{k+} \approx \epsilon_k \approx 0$  so that

$$E_{k+} \approx \epsilon_k + \frac{b_0^2}{\epsilon_k - \epsilon_{kf}} \Rightarrow u_k \approx -\frac{J_H}{b_0} v_k. \quad (12)$$

Using Eqs. (10), we then find  $Z \approx 1$  on the  $c$ -Fermi surface.

At the Fermi surface of the  $f$ -band on the other hand,  $Z = v_k^2$ . Also near this Fermi surface,  $|ek - \epsilon_{kf}| \approx t$  where  $t$  is the conduction electron bandwidth. We have assumed as is reasonable that  $t \gg J_H$ . Thus for the  $f$ -Fermi surface,

$$E_{k+} \approx \epsilon_k + \frac{b_0^2}{\epsilon_k - \epsilon_{kf}} \Rightarrow u_k \approx -\frac{t}{b_0} v_k. \quad (13)$$

This then gives

$$Z = v_k^2 \approx \left(\frac{b_0}{t}\right)^2. \quad (14)$$

Thus the quasiparticle residue stays non-zero on the  $c$ -Fermi surface while it decreases continuously to zero on the  $f$ -Fermi surface on moving from FL to FL\*. (The  $f$ -Fermi surface is “hot” while the  $c$ -Fermi surface is “cold”.)

Clearly the critical point is not a Fermi liquid.  $Z$  vanishes throughout the hot Fermi surface at the transition, and non-Fermi liquid behavior results. It is interesting to contrast this result with the spin-fluctuation model (Hertz-Moriya-Millis criticality) where the non-Fermi liquid behavior is only associated with some “hot” lines in the Fermi surface, and consequently plays a subdominant role.

Despite the vanishing quasiparticle weight  $Z$ , the effective mass  $m^*$  of the large Fermi surface state does not diverge at the transition in this mean-field calculation, because the electron self-energy is momentum-dependent. Physically, the quasiparticle at the hot Fermi surface is essentially made up of the  $f$ -particle for small  $b$ ; even when  $b$  goes to zero the  $f$ -particle (the spinon) continues to disperse due to the non-vanishing  $\chi_0$  term. Indeed the low-temperature specific heat  $C \sim \gamma T$  with  $\gamma$  non-zero in both phases. As we argue below, this is an artifact of the mean-field approximation and will be modified by fluctuations.

The detailed shape of the spinon Fermi surface in the FL\* phase (or the hot Fermi surface which derives from it in the FL phase) depends on the details of the lattice and the form of the local moment interactions. For the particular model discussed above, the spinon Fermi surface is perfectly nested. In more general situations, a non-nested spinon Fermi surface will obtain. In all cases, however, the volume of the spinon Fermi surface will correspond to one spinon per site.

#### IV. FLUCTUATIONS: MAGNETISM AND SINGULAR SPECIFIC HEAT

Fluctuation effects modify the picture obtained in the mean-field theory in several important ways. We first discuss fluctuation effects in the two phases. The heavy Fermi liquid phase is of course stable to fluctuations – their main effect being to endow the  $f$ -particle with a physical electric charge thereby making it an electron [36, 37]. Fluctuation effects are more interesting in the FL\* state, and are described by a U(1) gauge theory minimally coupled to the spinon Fermi surface (which continues to be essentially decoupled from the conduction electron small Fermi surface). This may be made explicit by parameterizing the fluctuations in the action in the FL\* phase as follows:

$$\chi_{rr'}(\tau) = e^{ia_{rr'}(\tau)} \chi_{0rr'}. \quad (15)$$

The action then becomes

$$\begin{aligned}
S &= S_c + S_f + S_{fc} + S_b, \\
S_c &= \int d\tau \sum_k \bar{c}_k (\partial_\tau - \epsilon_k) c_k, \\
S_f &= \int d\tau \sum_r \bar{f}_r (\partial_\tau - i a_0) f_r \\
&\quad - \sum_{\langle rr' \rangle} \chi_0 (e^{i a_{rr'}} \bar{f}_r f_{r'} + \text{h.c.}), \\
S_{cf} &= - \int d\tau \sum_r (b_r \bar{c}_r f_r + \text{h.c.}), \\
S_b &= \int d\tau \sum_r \frac{4|b_r|^2}{J_K}.
\end{aligned} \tag{16}$$

As usual, the field  $a_0$  is introduced to impose the constraint that there is one spinon per site and may be interpreted as the time component of the gauge field. By assumption  $b_r$  is not condensed. It is useful to start by completely ignoring all coupling between  $c$  and  $f$  fermions. The action for the  $f$  particles describes a Fermi surface of spinons coupled to a compact U(1) gauge field.

An important simplification for the three-dimensional systems of interest (as compared to  $d = 2$ ) is that the U(1) gauge theory admits a deconfined phase where the spinons potentially survive as good excitations of the phase. In what follows we will assume that the system is in such a deconfined phase. (This is formally justified in the same large- $N$  limit as the one for the mean field approximation.) This deconfined phase has a Fermi surface of spinons coupled minimally to a gapless “photon” (U(1) gauge field). (Due to the compactness of the underlying gauge theory, there is also a gapped monopole excitation.) Thus two static spinons interact with each other through an *emergent long range*  $1/r$  Coulomb interaction. Putting back a small coupling between the  $c$  and  $f$  particles will not change the deconfined nature of this phase. (In particular the monopole gap will be preserved.) This is the advocated U(1) FL\* phase.

### A. Specific heat

The coupling of the massless gauge photon to the spinon Fermi surface leads to several interesting modifications of the mean field results. First, consider the effect of the spatial components of the gauge field. It is useful to work in the gauge  $\vec{\nabla} \cdot \vec{a} = 0$  so that the vector potential is purely transverse. Unless otherwise stated, we assume a generic spinon Fermi surface (without flat portions) henceforth. Integrating out the spinons and expanding the resulting action to quadratic order gives the following well-known form for the propagator for these transverse gauge fluctuations:

$$D_{ij}(\vec{k}, i\omega_n) \equiv \langle a_i(\vec{k}, i\omega_n) a_j(-\vec{k}, -i\omega_n) \rangle$$

$$= \frac{\delta_{ij} - k_i k_j / k^2}{\Gamma |\omega_n| / k + \chi_f k^2}. \tag{17}$$

Here  $\Gamma, \chi_f$  are positive constants that are determined by the details of the spinon dispersion, and  $\omega_n$  is an imaginary Matsubara frequency. Note that the gauge fluctuations are overdamped in the small  $q$  limit. As was first shown in a different context by Holstein *et al.* [38] (and reviewed in Appendix D), this form of the gauge field action leads to a  $T \ln 1/T$  singularity in the low-temperature specific heat. Thus the specific heat coefficient  $\gamma = C/T$  diverges logarithmically at low temperature in the U(1) FL\* phase.

We also briefly mention the effect of the longitudinal (time-component) of the gauge field. This couples to the local  $f$  fermion density, and so its influence is very much like a repulsive density-density interaction. The longitudinal gauge field propagator has a structure very similar to that of a standard RPA density fluctuation propagator, and so does not lead to any non-Fermi liquid behavior.

### B. Magnetic instability

The repulsive interaction mediated by the longitudinal part of the gauge interaction can lead to various instabilities of the spinon Fermi surface. In particular, it is interesting to consider an SDW instability of the spinon Fermi surface. The resulting state will have magnetic long range order that could potentially have a weak moment as it is an SDW state that is formed out of the spinon Fermi surface. However, in contrast to the traditional view of the weak magnetism, here the SDW instability is *not* that of the large Fermi surface heavy Fermi liquid. Despite the occurrence of magnetic long range order, this magnetic state is far from conventional. Because the SDW order parameter is gauge neutral, the presence or absence of a SDW condensate has little substantive effect on the structure of the gauge fluctuations. Indeed, the latter remain as in the U(1) FL\* state, even after the magnetic order has appeared in the descendant U(1) SDW\* state. The spinons continue to be deconfined and are coupled to a gapless U(1) gauge field. Further, the monopole survives as a gapped excitation – this yields a sharp distinction with more conventional magnetic phases. These gauge excitations coexist with the gapless magnons associated with broken spin rotation invariance and with a Fermi surface of the conduction electrons. However, due to the broken translational symmetry in this state, there is no sharp distinction between small and large Fermi surfaces. So to reiterate, the exotic magnetic metal, dubbed U(1) SDW\*, emerges as a low-energy instability of the spinon Fermi surface of the parent U(1) FL\* state.

Different possibilities emerge for the formation of the spin density wave out of the parent U(1) FL\* phase, depending on the details of the spinon Fermi surface and the strength of the interactions driving the SDW instability. We enumerate some of them below:



- (A) Perfectly nested spinon Fermi surface:

In this case, arbitrarily weak interactions will drive an SDW instability. In the resulting state, the spinons are gapped. So upon integrating out the spinons, the effective action for the gauge field can be expanded safely in spatial and temporal gradients, with no long-range couplings. Gauge invariance now demands that these terms in the gauge field action have the standard Maxwell form. Consequently, the photon becomes a sharp propagating mode at low energies (below the spinon gap) with linear dispersion. Despite clearly being a distinct phase from conventional spin density wave metals, the experimental distinction is subtle.

- (B) Generic spinon Fermi surface, weak interaction:

For a generic spinon Fermi surface, the leading spin density wave instability (which will require an interaction strength beyond some threshold value) will be at a wavevector that matches one of the “ $2k_F$ ” wavevectors of the spinon Fermi surface. In the resulting state, a portion of the spinon Fermi surface (away from points connected by the ordering wavevector) survives intact. The damping of the gapless U(1) gauge fluctuations due to coupling to gapless spinons is preserved. Consequently the low-temperature specific heat will continue to behave as  $C(T) \sim T \ln(1/T)$ . Thus for this particular U(1) SDW\* state its non-Fermi liquid nature is readily manifested by specific heat measurements, providing a concrete example of a weak moment SDW metal with non-Fermi liquid thermodynamics at low temperature.

- (C) Generic spinon Fermi surface, strong interaction:

If the interactions are strong enough, even for a non-nested spinon Fermi surface, the spinons can develop a full gap with no portion of their Fermi surface remaining intact. The resulting phase is the same as that obtained in (A), and has a sharp propagating linear dispersing photon at low energies.

In Section VI we discuss experimental probes that can help distinguish these U(1) SDW\* phase from the conventional spin density wave metals.

### C. Mean-field theory with magnetism

In view of the possible occurrence of SDW phases we will now consider a modified mean-field theory which captures the magnetic instability at the mean-field level, but does no longer correspond to a large- $N$  saddle point. We will discuss the fully self-consistent solution of the mean-field equations for arbitrary temperature and external magnetic field.

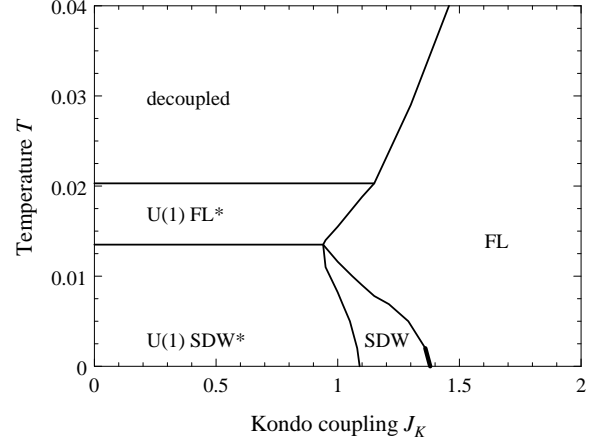


FIG. 4: Mean-field phase diagram of  $H_{\text{mf}}$  (18) on the cubic lattice, as function of Kondo coupling  $J_K$  and temperature  $T$ . Parameter values are electron hopping  $t = 1$ , Heisenberg interaction  $J_H = 0.1$ , decoupling parameter  $x = 0.2$ , and conduction band filling  $n_c = 0.7$ . Thin (thick) lines are second (first) order transitions. The “decoupled” phase is an artifact of the mean-field theory, and the corresponding transitions will become crossovers upon including fluctuations, as will the transition between the FL and U(1) FL\* phases; the transitions surrounding the SDW and SDW\* phases will of course survive beyond mean-field theory.

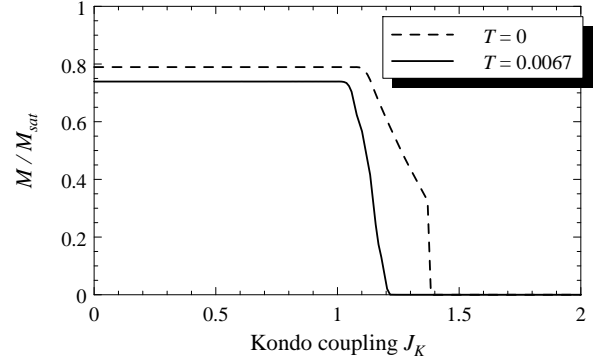


FIG. 5: Staggered magnetization determined from the mean-field solution  $H_{\text{mf}}$  (18). Parameter values are as in Fig. 4, the two curves correspond to two horizontal cuts of the phase diagram in Fig. 4. At  $T = 0$ , the first-order character of the SDW–FL transition is clearly seen. Note that smaller values of the decoupling parameter  $x$  yield smaller values of the magnetization in the SDW and SDW\* phases.

The mean-field Hamiltonian, written down explicitly for SU(2) symmetry, takes the following form:

$$\begin{aligned}
 H_{\text{mf}} = & \sum_k \epsilon_k c_{k\alpha}^\dagger c_{k\alpha} - \sum_{\langle rr' \rangle} (\chi_{rr'}^* f_{r\alpha}^\dagger f_{r'\alpha} + \text{h.c.}) \\
 & + \sum_r \mu_{f,r} f_{r\alpha}^\dagger f_{r\alpha} - \sum_r b_r (c_{r\alpha}^\dagger f_{r\alpha} + \text{h.c.})
 \end{aligned}$$

$$\begin{aligned}
& + \frac{1}{2} \sum_r (\vec{H}_{\text{eff},r} + \vec{H}_{\text{ext}}) \cdot f_{r\alpha}^\dagger \vec{\sigma}_{\alpha\alpha'} f_{r\alpha'} \\
& + \frac{1}{2} \vec{H}_{\text{ext}} \cdot \sum_r c_{r\alpha}^\dagger \vec{\sigma}_{\alpha\alpha'} c_{r\alpha'} + E_{\text{const}} \quad (18)
\end{aligned}$$

where  $\vec{H}_{\text{ext}}$  is the external field, and we have allowed for a spatial dependence of the mean-field parameters  $\mu_{f,r}$ ,  $\chi_{rr'}$ ,  $b_r$ ,  $\vec{H}_{\text{eff},r}$ . They have to be determined from the following equations:

$$1 = \langle f_{r\alpha}^\dagger f_{r\alpha} \rangle, \quad (19)$$

$$2b_r = J_K \langle c_{r\alpha}^\dagger f_{r\alpha} \rangle, \quad (20)$$

$$2\chi_{rr'} = (1-x)J_H \langle f_{r\alpha}^\dagger f_{r'\alpha} \rangle, \quad (21)$$

$$\vec{H}_{\text{eff},r} = xJ_H \sum_{r'} \vec{M}_{r'}, \quad \vec{M}_r = \frac{1}{2} \langle f_{r\alpha}^\dagger \vec{\sigma}_{\alpha\alpha'} f_{r\alpha'} \rangle, \quad (22)$$

where the last sum runs over the nearest neighbors  $r'$  of site  $r$ . We have introduced a parameter  $x$  which allows to control the balance between ordered local-moment magnetism and spin-liquid behavior of the  $f$  electrons. A value  $x = 1/2$  would correspond to an unrestricted Hartree-Fock treatment of the original Heisenberg interaction; we will employ values  $x < 1/2$  in order to model a *weak* magnetic instability of the spinon Fermi surface state. The constant piece of the Hamiltonian reads

$$\begin{aligned}
E_{\text{const}} &= - \sum_r \mu_{f,r} + \sum_r \frac{2b_r^2}{J_K} \\
&+ \sum_{rr'} \frac{2|\chi_{rr'}|^2}{(1-x)J_H} - \frac{1}{2} \sum_r \vec{H}_{\text{eff},r} \cdot \vec{M}_r. \quad (23)
\end{aligned}$$

For simplicity, we consider a simple cubic lattice, and assume a tight-binding dispersion for the conduction electrons,  $\epsilon_k = -2t \sum_{a=1,2,3} \cos(k_a) - \mu_c$ , where  $\mu_c$  controls the conduction band filling. The mean-field equations can be self-consistently solved using a large unit cell, allowing for spatially inhomogeneous phases [39]. In this section we restrict our attention to mean-field solutions where the  $\chi_{rr'} = \chi_0$  fields are real (time-reversal invariant) and obey the full lattice symmetries, and  $b_r = b_0$  is site-independent. We employ a  $2 \times 1$  unit cell, then antiferromagnetism is characterized by  $\vec{M}_r \cdot \hat{x} = M_s \exp(i\mathbf{Q} \cdot \mathbf{r})$  where  $\mathbf{Q} = (\pi, \pi, \pi)$  is the antiferromagnetic wavevector, and  $\hat{x}$  is the magnetization axis (which is arbitrary in zero external field).

In Fig. 4 we show a phase diagram obtained from self-consistently solving (18) together with the above mean-field equations at zero external magnetic field. A U(1) FL\* phase with  $b_0 = 0$  and  $\chi_0 \neq 0$  is realized at intermediate temperatures. As expected, it is unstable to magnetic order at low  $T$ , resulting in a U(1) SDW\* ground state for small  $J_K$  – this phase has in addition  $M_s \neq 0$ . For the present parameter values, the spinon Fermi surface is gapped out in the SDW\* phase. Increasing  $J_K$  drives the system into the FL phase with  $b_0 \neq 0$ ,  $\chi_0 \neq 0$ , and  $M_s = 0$ ; at low temperatures a conventional SDW

phase intervenes where all  $b_0$ ,  $\chi_0$ ,  $M_s$  are non-zero. Note that the transition between FL and SDW is weakly first order at low temperatures. At high temperature, the mean-field theory only has a “decoupled” solution with  $b_0 = \chi_0 = M_s = 0$  – this decoupling is a well-known mean-field artifact and reflects the presence of incoherent excitations.

In the FL phase, the above mentioned Lifshitz transition occurs at  $J_K \approx 1.7$  in the low-temperature limit, *i.e.*, for  $J_K > 1.7$  only a single Fermi surface sheet remains. Note that this transition does not lead to strong singularities in the mean-field parameters.

The staggered magnetization of the SDW and SDW\* states as determined from the mean-field solution are shown in Fig. 5; we can expect that fluctuation corrections will significantly reduce these mean-field values. We have also studied different values of the decoupling parameter  $x$ ; in particular smaller values of  $x$  lead to a suppression of ordered magnetism in favor of the non-magnetic FL\* state, *i.e.*, the SDW instability of FL\* is shifted to lower temperatures (and becomes completely suppressed at small  $x$ ); similarly, the ordered moment in the SDW phases is decreased with decreasing  $x$ .

Interesting physics obtains when an external magnetic field is turned on, and the corresponding mean-field phase diagram is discussed in Appendix C.

## V. FLUCTUATIONS NEAR THE FERMI VOLUME CHANGING TRANSITION

We now turn to the effects of fluctuations beyond the mean-field theory at the phase transition between the FL and U(1) FL\* phases. In mean-field theory, this transition occurs through the condensation of the slave boson field  $b$ . Such a condensation survives as a sharp transition beyond mean-field only when  $T = 0$ .

We begin by observing that in the mean-field theory all the important changes near the transition occur at the hot Fermi surface. The cold Fermi surface (essentially made up of  $c$ -particles) plays a spectator role. We therefore integrate out the  $c$ -fields completely from the action in Eq. (16) to obtain an effective action involving the  $b$ ,  $f$  and gauge fields alone. We also partially integrate out  $f$  excitations well away from the hot Fermi surface: this changes the  $b$  effective action from the simple local term in (16), and endows it with frequency and momentum dependence. In this manner we obtain the following effective action at long distance and time scales:

$$S = S_b + S_f, \quad (24)$$

$$\begin{aligned}
S_b &= \int d\tau d^3r \left[ \bar{b} \left( \partial_\tau - \mu_b - ia_0 - \frac{(\vec{\nabla}_r - i\vec{a})^2}{2m_b} \right) b \right. \\
&\quad \left. + \frac{u}{2} |b|^4 + \dots \right], \quad (25)
\end{aligned}$$

and  $S_f$  has the same form as in (16). Notice that the

$b$  field has become a propagating boson, with the same terms in the action as a microscopic canonical boson: here these terms arise from a  $(b, f)$  fermion polarization loop integrated well away from the  $f$  Fermi surface. The parameters  $\mu_b, m_b$  may be interpreted as the chemical potential and mass of the bosons respectively. The  $(b, f)$  fermion loop will also lead to higher time and spatial gradient terms as well as a density-density coupling between  $b$  and  $f$  in (24), but all these are formally irrelevant near the quantum critical point of interest.

A key feature of (24), induced by taking the spatial and temporal continuum limit, is that we have lost information on the compactness of the  $U(1)$  gauge field  $a$ , *i.e.*, the continuum action is now no longer periodic under  $a_{rr'} \rightarrow a_{rr'} + 2\pi$ , as was the case for the lattice action (16). The  $U(1)$  gauge field is now effectively non-compact, and consequently monopole excitations have been suppressed. The monopole gap is finite in the  $U(1)$  FL\* phase (which is the analog of the “Coulomb” phase of the compact gauge theory) [40]. In the FL phase, the monopoles do not exist – they are confined to each other. This occurs due to the condensation of the boson field. However, the monopole gap is not expected to close at the transition [42], and so neglecting the compactness of the gauge field is permissible. Indeed, the continuum action (24) provides a satisfactory description of the critical properties of the FL to  $U(1)$  FL\* transition at  $T = 0$ . However, as we noted in the caption of Fig 1, the compactness of the gauge field is crucial in understanding the absence of a  $T > 0$  phase transition above the FL phase [21].

The action in Eq. (24) above is similar to that popular in gauge theory descriptions [22, 23] of the normal state of optimally doped cuprates but with some crucial differences. Here the chemical potential of the bosons is fixed while in Refs. 22, 23 the boson density was fixed; as we will see below, this significantly modifies the physical implications of the critical theory, and the nature of the non-Fermi liquid critical singularities as  $T > 0$ . Furthermore, we are interested specifically in  $d = 3$ , as opposed to the  $d = 2$  case considered in Refs. 22, 23.

The phase diagram of the action (24) was sketched in Fig 1. The horizontal axis, represented in Fig 1 by  $J_K$ , is now accessed by varying  $\mu_b$ . Without any additional (formally irrelevant) second-order time derivative terms for  $b$  in the action, the quantum critical point between the FL and  $U(1)$  FL\* phases occurs precisely at  $\mu_b = 0$ ,  $T = 0$ . We will now discuss the physical properties in the vicinity of this critical point first at  $T = 0$ , and then at  $T > 0$ , followed by an analysis of transport properties using the quantum Boltzmann equation in Section V C. The final subsection V D will comment on the effect of the SDW or SDW\* phases that may appear at very low temperatures (these are not shown in Fig. 1, but sketched in Fig. 2).

## A. Zero temperature

In a mean-field analysis of (24), we see that the FL\* phase (the “Coulomb” phase of the gauge theory) obtains for  $\mu_b < 0$  with  $\langle b \rangle = 0$ , while the FL phase (the “Higgs” phase of the gauge theory) obtains for  $\mu_b > 0$ .

Consider fluctuations for  $\mu_b < 0$  in the FL\* phase. Here, there are no bosons in the ground state, and all self-energy corrections associated with the quartic coupling  $u$  vanish [41]. The gauge field propagator is given by (17), and this does contribute a non-zero boson self energy. At small momenta  $p$  and imaginary frequencies  $\epsilon$ , the boson self-energy has the structure (determined from a single gauge-boson exchange process, as in Refs. 22, 23)

$$\Sigma_b(k, i\epsilon) \sim k^2(1 + c_1|\epsilon| \ln(1/|\epsilon|) + \dots), \quad (26)$$

where  $c_1$  is some constant. Apart from terms which renormalize the boson mass  $m_b$ , these self-energy corrections are less relevant than the bare terms in the action, and so can be safely neglected near the critical point. Notice also that  $\Sigma_b(0, 0) = 0$ , and so the quantum critical point remains at  $\mu_b = 0$ .

The critical exponents can now be determined as in Refs. 20, 41, and are simply those of the mean-field theory of (24):

$$\nu = 1/2 \quad ; \quad z = 2 \quad ; \quad \eta = 0. \quad (27)$$

As in (26) we can also determine the fate the boson quasi-particle pole as influenced by the gauge fluctuations; we obtain

$$\text{Im}\Sigma_b\left(k, \epsilon = \frac{k^2}{2m_b}\right) \sim \text{sgn}(\epsilon)\epsilon^2 \ln(1/|\epsilon|). \quad (28)$$

The boson lifetime is clearly longer than its energy, and this pole remains well defined. Finally, we recall our statement in Section IV A that the gauge fluctuations lead to a  $T \ln(1/T)$  specific heat in the FL\* phase, with a diverging  $\gamma$  co-efficient. This behavior remains all the way up to, and including, the critical point. Parenthetically, we note that the same calculation in  $d = 2$  dimensions will yield  $C \propto T^{2/3}$ .

We turn next to  $\mu_b > 0$ , in the FL phase. Here the bosons are condensed, and (26) or explicit calculations show that

$$\langle b \rangle \equiv b_0 \sim (\mu_b)^{1/2} \sim (J_K - J_{Kc})^{1/2}, \quad (29)$$

where  $J_{Kc}$  is the position of the critical point in Fig 1. The transverse gauge field propagator may be obtained as in Section IV A by integrating out both the bosons and fermions and expanding the resulting action to quadratic order; the boson condensate leads to a “Meissner” term in the gauge propagator so that (17) is replaced by

$$\begin{aligned} D_{ij}(\vec{k}, i\omega_n) &\equiv \langle a_i(\vec{k}, i\omega_n) a_j(-\vec{k}, -\omega_n) \rangle \\ &= \frac{\delta_{ij} - k_i k_j / k^2}{\Gamma|\omega_n|/k + \chi_f k^2 + \rho_s}. \end{aligned} \quad (30)$$

Here  $\rho_s$  is the boson “superfluid density”, and we have  $\rho_s \sim b_0^2$ . The presence of such a Meissner term cuts off the singular gauge fluctuations. The divergence of the specific heat coefficient  $\gamma(T)$  as a function of temperature at the critical point implies that it diverges at  $T = 0$  on approaching the transition from the FL side. As shown in Appendix D, this is indeed the case, and we find that  $\gamma$  diverges as  $\gamma \sim \ln(1/b_0)$ . In experiments, such a diverging  $\gamma$  is sometimes interpreted as a diverging effective mass. Importantly, the divergence of  $\gamma$  is unrelated to the singularity in the quasiparticle residue on the “hot” Fermi sheet,  $Z$ , which obeys  $Z \sim b_0^2$  as shown in (14), and so vanishes linearly as a function of  $J_K - J_{Kc}$ .

### B. Non-zero temperatures

A crucial change at  $T > 0$  is that it is now no-longer true that  $\Sigma_b(0,0) = 0$  in a region with  $\langle b \rangle = 0$ . Instead, as in earlier studies of the dilute Bose gas [19, 20], we have

$$\begin{aligned} \Sigma_b(0,0) &= 2u \int \frac{d^d k}{(2\pi)^d} \frac{1}{\exp[k^2/(2m_b T)] - 1} \\ &= u \frac{\zeta(3/2)}{4\pi^{3/2}} (2m_b T)^{3/2} \quad \text{in } d = 3 \end{aligned} \quad (31)$$

This behavior determines the crossover phase boundaries shown in Fig 1. The physical properties are determined by the larger of the two “mass” terms in the  $b$  Green’s function,  $|\mu_b|$  or  $\Sigma_b(0,0)$  – consequently, the crossover phase boundaries in Fig. 1 lie at  $T \sim |\mu_b|^{2/3} \sim |J_K - J_{Kc}|^{2/3}$ . These boundaries separate the U(1) FL\* region at low  $T$  and  $\mu_b < 0$ , and the FL region at low  $T$  and  $\mu_b > 0$ , from the intermediate quantum critical region. Note that there is no phase transition in the FL region at  $T > 0$ : this is due to the compactness of the underlying U(1) gauge theory, and the fact that the “Higgs” and “confining” phases are smoothly connected in a compact U(1) gauge theory in three total dimensions [21].

We now briefly comment on the nature of the electrical transport in the three regions of Fig 1. The behavior is quite complicated, and we will first highlight the main results by simple estimates in the present subsection. A more complete presentation based upon the quantum Boltzmann equation appears in Section V C.

The conventional FL region is the simplest, with the usual  $T^2$  dependence of the resistivity—the gauge fluctuations are quenched by the “Meissner effect”.

In the U(1) FL\* region, there is an exponentially small density of thermally excited  $b$  quanta, and so the boson conductivity  $\sigma_b$  is also exponentially small. As in earlier work [43], the resistances of the  $b$  and  $f$  quanta add in series, and so the total  $b$  and  $f$  conductivity remains exponentially small. The physical conductivity is therefore dominated by that of the  $c$  fermions, which again has a conventional  $T^2$  dependence.

Finally, we comment on the transport in the quantum critical region. This we will estimate following the

method of Ref. 22, with a more complete calculation appearing in the following subsection. A standard Fermi’s Golden rule computation of scattering off low-energy gauge fluctuations shows that a boson of energy  $\epsilon$  has a transport scattering rate

$$\frac{1}{\tau_{\text{btr}}(\epsilon)} \sim T\sqrt{\epsilon} \quad (32)$$

for energies  $\epsilon \ll T^{2/3}$ . From this, we may obtain the boson conductivity by inserting in the expression

$$\sigma_b \sim \int d^3 k \tau_{\text{btr}}(\epsilon_{bk}) k^2 \left( -\frac{\partial n(\epsilon_{bk})}{\partial \epsilon_{bk}} \right) \quad (33)$$

where  $n(\epsilon) = 1/(e^{\epsilon/T} - 1)$  is the Bose function, and  $\epsilon_{bk} = k^2/(2m_b) + \Sigma_b(0,0) = k^2/(2m_b) + c_2 T^{3/2}$  for some constant  $c_2$ . Estimating the integral in (33) we find that there is an incipient logarithmic divergence at small  $k$  which is cutoff by  $\Sigma_b(0,0) \sim T^{3/2}$ , and so  $\sigma_b$  diverges logarithmically with  $T$ :

$$\sigma_b \sim \ln(1/T). \quad (34)$$

There are no changes to the estimate of the  $f$  conductivity from earlier work [22, 23], and we have  $\sigma_f \sim T^{-5/3}$ . Using again the composition rule of Ref. 43, we see that the asymptotic low-temperature physical conductivity is dominated by the behavior in (34).

As an aside, we note that for the theory (24) in *two* spatial dimensions the result of Eq. (34) continues to hold, whereas the fermion part becomes  $\sigma_f \sim T^{-4/3}$ . This implies that the asymptotic low- $T$  physical conductivity is dominated by (34) in  $d = 2$  as well.

### C. Quantum Boltzmann equation

We now address electrical transport properties of the theory (24) in more detail, using a quantum Boltzmann equation. The analysis is in the same spirit as the work of Ref. 44 but, as we have discussed in Section I A, the variation in the boson density as a function of temperature leads to very different physical properties, and requires a distinct analysis of the transport equation.

We saw in Section V B that the electrical conductivity was dominated by the  $b$  boson contribution, and so we focus on the time ( $t$ ) dependence described by the distribution function

$$f(\vec{k}, t) = \langle b_k^\dagger(t) b_k(t) \rangle \quad (35)$$

In the absence of an external (physical) electric field  $\vec{E}$ , we have the steady state value  $f(\vec{k}, t) = f_0(k)$  with

$$f_0(k) \equiv \frac{1}{\exp[(k^2/(2m_b) - \mu_b + \Sigma_b(0,0))/T] - 1}, \quad (36)$$

with  $\Sigma_b(0,0)$  given in (31). The transport equation in the presence of a non-zero  $\vec{E}(t)$  can be derived by standard means, and most simply by an application of Fermi’s

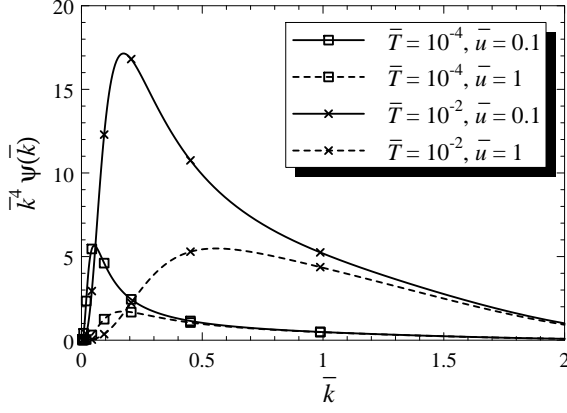


FIG. 6: Plot of the function  $\bar{k}^4 \psi(\bar{k})$  for a few values of the reduced temperature  $\bar{T}$  and the interaction parameter  $\bar{u}$  (40).  $\psi(\bar{k})$  is defined in Eqs. (38) and (41), and has been obtained from the numerical solution of the quantum Boltzmann equation (42).

golden rule. The bosons are assumed to scatter off a fluctuating gauge field with a propagator given by (17) or (30), and this yields the equation

$$\begin{aligned} \frac{\partial f(\vec{k}, t)}{\partial t} + \vec{E}(t) \cdot \frac{\partial f(\vec{k}, t)}{\partial \vec{k}} = & \\ - \int_{-\infty}^{\infty} \frac{d\Omega}{\pi} \int \frac{d^d q}{(2\pi)^d} \text{Im} \left[ \frac{k_i D_{ij}(\vec{q}, \Omega) k_j}{m_b^2} \right] & \\ \times (2\pi) \delta \left( \frac{k^2}{2m_b} - \frac{(\vec{k} + \vec{q})^2}{2m_b} - \Omega \right) & \\ \times \left[ f(\vec{k}, t)(1 + f(\vec{k} + \vec{q}, t))(1 + n(\Omega)) \right. & \\ \left. - f(\vec{k} + \vec{q}, t)(1 + f(\vec{k}, t))n(\Omega) \right] & \end{aligned} \quad (37)$$

where  $n(\Omega)$  is the Bose function at a temperature  $T$  as above.

We will now present a complete numerical solution of (37) for the case of a weak, static electric field, to linear order in  $\vec{E}$ . The analysis near the quantum critical point parallels that of Ref. 45, with the main change being that instead of the critical scattering appearing from the boson self-interaction  $u$ , the dominant scattering is from the gauge field fluctuations (note, however, that it is essential to include the interaction  $u$  to first order in the self-energy shift in (36)). We write

$$f(\vec{k}, t) = f_0(k) + \vec{k} \cdot \vec{E} f_1(k), \quad (38)$$

where notice that  $f_1$  depends only on the modulus of  $k$  and is independent of  $t$ . We now have to insert (38) into the transport equation (37) and the expression for the electrical current

$$\vec{J}(t) = \int \frac{d^d k}{(2\pi)^d} \frac{\vec{k}}{m_b} f(\vec{k}, t), \quad (39)$$

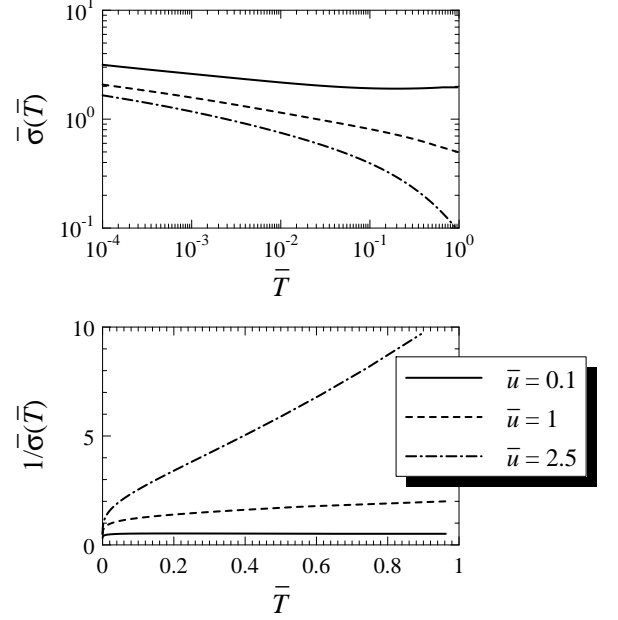


FIG. 7: Scaling function for the boson conductivity,  $\bar{\sigma} = \sigma_b/(m_b \chi_f)$ , as function of the reduced temperature  $\bar{T}$  for different values of the interaction parameter  $\bar{u}$  (40). The results are obtained from the numerical solution of the quantum Boltzmann equation (42) together with (43). Top panel: conductivity  $\bar{\sigma}(\bar{T})$  on a log-log scale. Bottom panel: resistivity  $1/\bar{\sigma}(\bar{T})$  on a linear scale.

linearize everything in  $\vec{E}$ , and so determine the proportionality between  $\vec{J}$  and  $\vec{E}$ .

It is useful to re-write the equations in dimensionless quantities  $\bar{\Omega} = \Omega/T$ ,  $\bar{k} = k/\sqrt{2m_b T}$ ,  $\bar{\sigma} = \sigma_b/(m_b \chi_f)$ . Then it is easy to see that the solution of the quantum Boltzmann equation at the critical coupling,  $\mu_b = 0$ , is characterized by two parameters,

$$\begin{aligned} \bar{T} &= \frac{\chi_f^2}{\Gamma^2} (2m_b)^3 T, \\ \bar{u} &= u \frac{\zeta(3/2)}{4\pi^{3/2}} \frac{\Gamma}{\chi_f}, \end{aligned} \quad (40)$$

where  $\bar{T}$  is a reduced temperature, and  $\bar{u}$  parametrizes the temperature dependence of the effective “mass” of the bosons from Eq. (31);  $\Gamma$  and  $\chi_f$  are the parameters of the gauge propagator (17). The linearized form of the Boltzmann equation (37) for the function

$$f_1(k) \equiv \psi(k/\sqrt{2m_b T}) \quad (41)$$

is obtained as

$$-f'_0(\bar{k}) = \int_0^\infty d\bar{k}_1 [K_1(\bar{k}, \bar{k}_1)\psi(\bar{k}) + K_2(\bar{k}, \bar{k}_1)\psi(\bar{k}_1)] \quad (42)$$

with  $f'_0(x) = \partial/(\partial x^2)[\exp(x^2 + \bar{u}\sqrt{T}) - 1]^{-1}$ ; the expressions for the functions  $K_{1,2}$  are given in Appendix E.

From the solution of Eq. (42) one obtains the conductivity according to

$$\bar{\sigma}(\bar{T}, \bar{u}) = \frac{1}{6\pi^2\sqrt{\bar{T}}} \int_0^\infty d\bar{k} \bar{k}^4 \psi(\bar{k}). \quad (43)$$

The integral equation (42) was solved by straightforward numerical iteration on a logarithmic momentum grid. We show sample solutions for the function  $\bar{k}^4 \psi(\bar{k})$  in Fig. 6. The final results for the scaling function of the conductivity are displayed in Fig. 7. For small temperatures, the logarithmic divergence of  $\sigma_b(T)$  announced in Eq. (34) is clearly seen; for larger temperatures the conductivity is exponentially suppressed due to the temperature-dependent boson mass. In the crossover region, the results could be fitted with a power law over a restricted temperature range of roughly one decade, however, no extended power-law regime emerges. In comparison with experiments, one has to keep in mind that the physical resistivity is given by a sum of boson and fermion resistivities, and that the logarithmically decreasing low-temperature part of  $1/\sigma_b(T)$  cannot be easily distinguished from a residual resistivity arising from impurities.

#### D. SDW order

Our discussion so far has focused primarily on the crossover between the FL to U(1) FL\* phases, as this captures the primary physics of the Fermi volume changing transition. At low  $T$ , we discussed in Section IV B that the longitudinal part of the gauge fluctuations may induce SDW order on the spinon Fermi surface of the FL\* phase (leading to the SDW\* phase). On the FL side of the transition, the gauge fluctuations are formally gapped by the Anderson-Higgs mechanism. They will, however, still mediate a repulsive (though finite ranged) interaction between the quasiparticles at the hot Fermi surface. Furthermore the shape of the hot Fermi surface evolves smoothly from the spinon Fermi surface if the FL\* phase. Consequently, it is to be expected that the SDW order will continue into the FL region up to some distance away from the transition. Thus it seems unlikely that there will be a direct transition from SDW\* to FL at zero temperature. The actual situation then has some similarities to the mean-field phase diagram in Fig 4. However, fluctuations will strongly modify the positions of the phase boundaries, and we expect that the U(1) FL\* region actually occupies a larger portion of the phase diagram. Also there is no sharp transition between the FL and U(1) FL\* regions (unlike the mean-field situation in Fig 4), and there is instead expected to be a large intermediate quantum-critical region as shown in Fig. 2.

## VI. EXPERIMENTAL PROBES OF THE U(1) SDW\* STATE

In this Section, we discuss experimental signatures of the U(1) SDW\* phase focusing particularly on the distinctions with more conventional SDW metals.

We begin by considering a U(1) SDW\* phase in which a portion of the spinon Fermi surface remains intact. As discussed in Section IV, the coupling between the gapless spinons and the gauge field leads to singularities in the low-temperature thermodynamics in this phase. In particular the specific heat behaves as  $C(T) \sim T \ln(1/T)$  at low temperature. Thus this phase is readily distinguished experimentally from a conventional SDW. Electrical transport in this U(1) SDW\* phase will be through the conduction electrons with no participation from the spinons. Thus electrical transport will be Fermi liquid-like. In contrast thermal transport will receive contributions from both the conduction electrons and the gapless spinons. Consequently the thermal conductivity will be in excess of that expected on the basis of the Wiedemann-Franz law with the free electron Lorenz number.

The distinction with conventional SDW phases is much more subtle for U(1) SDW\* phases where the spinons have a full gap. In this case, there is a propagating gapless linear dispersing photon which is sharp. The presence of these gapless photon excitations potentially provides a direct experimental signature of this phase. It is extremely important to realize that the emergent gauge structure of a fractionalized phase is completely robust to all local perturbations, and is not to be confused with any modes associated with broken symmetries. Thus despite its gaplessness the photon is not a Goldstone mode. In fact, the gaplessness of the photon is *protected* even if there are small terms in the microscopic Hamiltonian that break global spin rotation invariance. Being gapless with a linear dispersion, the photons will contribute a  $T^3$  specific heat at low  $T$  which will add to similar contributions from the magnons and the phonons of the crystal lattice. In addition, the conduction electrons will contribute a linear  $T$  term. The phonon contribution is presumably easily subtracted out by a comparison between the heavy Fermi liquid and magnetic phases. To disentangle the magnon and photon contributions, it may be useful to exploit the robustness of the photons to perturbations. Thus for materials with an easy-plane anisotropy, application of an in-plane magnetic field will gap out the single magnon, but the photon will stay gapless and will essentially be unaffected (at weak fields). Thus careful measurements of field-dependent specific heat may perhaps be useful in deciding whether the U(1) SDW\* phase is realized.

Finally, quasi-elastic Raman scattering has been suggested as a probe of the U(1) gauge field fluctuations [46] in the context of the cuprates—the same prediction applies essentially unchanged here to the fractionalized phases in  $d = 3$ .

Conceptually the cleanest signature of the U(1) SDW\*

phase would be detection of the gapped monopole. However at present we do not know how this may be directly done in experiments. Designing such a “monopole detection” experiment is an interesting open problem.

## VII. DISCUSSION

The primary question which motivates this paper is how to reconcile a weak moment magnetic metal with non-Fermi liquid behavior close to the transition to the Fermi liquid. We have explored one concrete route toward such a reconciliation. The  $U(1)$  SDW\* magnetic states discussed in this paper may be dubbed spin-charge separated spin density wave metals. They constitute a class distinct from both the conventional spin density wave metal and the local-moment metal mentioned in the Introduction. However, they share a number of similarities with both conventional metals. Just as in the conventional local-moment metal, in the  $U(1)$  SDW\* state the local moments do not participate in the Fermi surface. Despite this the ordering moment may be very small. Indeed this state may be viewed as a spin density wave that has formed out of a parent non-magnetic metallic state with a “small Fermi surface”. This parent state is a fractionalized Fermi liquid in which the local moments have settled into a spin liquid and essentially decoupled from the conduction electrons. The spinons of the spin liquid form a Fermi surface which undergoes the SDW transition – this transition does not affect the deconfinement property of the gauge field, because the SDW order parameter is gauge neutral and thus does not effectively couple to the gauge field excitations.

We showed that in the region of evolution from this state to the conventional Fermi liquid, non-Fermi liquid behavior obtains (at least at intermediate temperatures). We also argued that the underlying transition that leads to this non-Fermi liquid physics is the Fermi volume changing transition from FL to FL\*. Despite the jump in the Fermi volume, this transition is continuous and characterized by the vanishing of the quasiparticle residue  $Z$  on an entire sheet of the Fermi surface (the “hot” Fermi surface) on approaching the transition from the FL side.

A specific heat that behaves as  $T \ln(1/T)$  is commonly observed in a variety of heavy-fermion materials close to the transition to magnetism. In the context of the ideas explored in this paper, such behavior of the specific heat is naturally obtained in *three-dimensional* systems. A small number of heavy-fermion materials exhibit such a singular specific heat even in the presence of long-ranged magnetic order. As we have emphasized, precisely such non-Fermi liquid specific heat obtains in one of the exotic magnetic metals discussed in this paper (the  $U(1)$  SDW\* phase with a partially gapped spinon Fermi surface). It would be interesting to check for violations of the Wiedemann-Franz law at low temperature in such materials.

A general point emphasized in this paper is that the observed non-Fermi liquid physics near the onset of magnetism actually has little to do with fluctuations of the magnetic order parameter. Rather we propose that the non-Fermi liquid physics is associated with the destruction of the large Fermi surface. The concrete realization of this picture explored in this paper is that the destruction of the large Fermi surface leads to a fractionalized Fermi liquid which eventually (at low temperature) develops spin density wave order. As we discussed extensively, the resulting spin density wave state is an exotic magnetic metal.

It is also of interest to consider a different scenario in which the small Fermi surface state is unstable at low temperature toward *confinement* of spinons and magnetic order. It is particularly interesting to consider such a scenario in  $d = 2$ . The physics of the Fermi-volume changing fluctuations is again described by a theory of condensation of a slave boson field coupled to a Fermi surface of spinons by a  $U(1)$  gauge field. For a non-compact  $U(1)$  gauge field, such a theory has a number of interesting properties. As noticed by Altshuler *et al.* [47], the spin susceptibility at extremal wavevectors of the spinon Fermi surface have (possibly divergent) singularities due to the gauge fluctuations. Indeed the spin physics of this model is critical and described by a non-trivial fixed point. The dynamical susceptibility at these extremal wavevectors and at a frequency  $\omega$  is expected to satisfy  $\omega/T$  scaling. For a general spinon Fermi surface these extremal wavevectors will chart out one-dimensional lines in the Brillouin zone at which critical scattering will be seen in inelastic neutron scattering. A spin density wave instability can develop out of this critical state at a particular extremal wavevector where the amplitude of the diverging susceptibility is the largest. Arguments very similar to those in Section VB also show that transport will be governed by non-Fermi liquid power laws in this theory.

There is a striking *qualitative* resemblance between these results and the experiments on  $\text{CeCu}_{6-x}\text{Au}_x$ . At the critical Au concentration neutron scattering experiments see critical scattering on lines in the Brillouin zone satisfying  $\omega/T$  scaling [5]. Magnetic ordering occurs at particular wavevectors on this line. Furthermore, empirically the spin fluctuations appear to be quasi two-dimensional, suggesting that the ideas sketched above may indeed be relevant. We note that they significantly differ from earlier proposals to explain the behavior of  $\text{CeCu}_{6-x}\text{Au}_x$  [48]. As mentioned in the text, the specific heat in the  $d = 2$  quantum critical region will have the form  $C/T \sim T^{-1/3}$ ; interestingly, such a behavior has been observed in  $\text{YbRh}_2\text{Si}_2$  in the low-temperature regime near a quantum-critical point [49]. On the theoretical front, there are a number of conceptual issues [50] related to the legitimacy of ignoring the compactness of the gauge field in  $d = 2$ . Developing a more concrete theoretical description of these general ideas is an interesting challenge for future work.

### Acknowledgments

We thank P. Coleman, M.P.A. Fisher, E. Fradkin, A. Georges, L. Ioffe, Y.-B. Kim, G. Kotliar, A. Millis, N. Prokof'ev, T. M. Rice, Q. Si, M. Sigrist, A. Tsvelik, and X.-G. Wen for useful discussions. T.S. is particularly grateful to Patrick Lee for a number of enlightening conversations that clarified his thinking. This research was supported by the MRSEC program of the US NSF under grant number DMR-0213282 (T.S.), by US NSF Grant DMR 0098226 (S.S.), and by the DFG Center for Functional Nanostructures at the University of Karlsruhe (M.V.). T.S. also acknowledges funding from the NEC Corporation, and the Alfred P. Sloan Foundation and the hospitality of Harvard University where part of this work was done.

### APPENDIX A: OSHIKAWA'S ARGUMENT AND TOPOLOGICAL ORDER

Oshikawa has presented [51] an elegant non-perturbative argument demonstrating that the volume of the Fermi surface is determined by the total number of electrons in the system. In our previous work [11], and in the present paper, we have argued for the existence of a non-magnetic FL\* state with a different Fermi surface volume. As we discussed earlier [11], this apparent conflict is resolved when we allow for global topological excitations in Oshikawa's analysis; such excitations emerge naturally in the gauge theories we have discussed for the FL\* state. In other words, Oshikawa's argument implies that violation of Luttinger's theorem must be accompanied by topological order.

In this Appendix, we briefly recall the steps in Oshikawa's argument, and show how it can be modified to allow for a small Fermi surface in a FL\* state. As far as possible, we follow the notation of Oshikawa's paper [51].

For definiteness, consider a two-dimensional Kondo lattice with a unit cell of lengths  $a_x, a_y$ . The ground state is assumed to be non-magnetic, with equal numbers of up and down spin electrons. Place it on a torus of lengths  $L_x, L_y$ , with  $L_x/a_x, L_y/a_y$  co-prime integers. Adiabatically insert a flux  $\Phi = 2\pi$  ( $\hbar = c = e = 1$ ) into one of the holes of the torus (say the one enclosing the  $x$  circumference), acting only on the up-spin electrons. Then the initial and final Hamiltonians are related by a unitary transformation generated by

$$U = \exp\left(\frac{2\pi i}{L_x} \sum_r n_{r\uparrow}\right) \quad (\text{A1})$$

where  $n_{r\uparrow}$  is the number operator of all electrons (including the local moments) with spin up on the site  $r$ . After performing the unitary transformation to make the final Hamiltonian equivalent to the initial Hamiltonian, the final and initial states are found to have a total crystal

momentum which differs by

$$\Delta P_x = \frac{2\pi}{L_x} \frac{L_x L_y}{v_0} \frac{\rho_a}{2} \left( \text{mod} \frac{2\pi}{a_x} \right) \quad (\text{A2})$$

where  $v_0 = a_x a_y$  is a volume of a unit cell, the second factor on the r.h.s. counts the number of unit cells in the system, and  $\rho_a = 2\rho_{a\uparrow}$  is the mean number of electrons in every unit cell. Clearly the crystal momentum is defined modulo  $2\pi/a_x$ , and hence the modulus in (A2).

Now imagine computing the change in crystal momentum by studying the response of the quasiparticles to the inserted flux. As shown by Oshikawa, the quasiparticles associated with a Fermi surface of volume  $\mathcal{V}$  lead to a change in momentum which is

$$\Delta P_x^q = \frac{2\pi}{L_x} \frac{\mathcal{V}}{(2\pi)^2/(L_x L_y)} \left( \text{mod} \frac{2\pi}{a_x} \right), \quad (\text{A3})$$

where the second factor on the r.h.s. counts the number of quasiparticles within the Fermi surface. Equating  $\Delta P_x$  and  $\Delta P_x^q$ , and the corresponding expressions for  $\Delta P_y$  and  $\Delta P_y^q$ , Oshikawa obtained the conventional Luttinger theorem, which applies to the volume  $\mathcal{V} = \mathcal{V}_{FL}$  of the Fermi surface in the FL state

$$2 \frac{v_0}{(2\pi)^2} \mathcal{V}_{FL} = \rho_a \pmod{2} \quad (\text{A4})$$

In the FL\* state, there are additional low-energy excitations of the local moments that yield an additional topological contribution to the change in crystal momentum. Indeed, the influence of an insertion of flux  $\Phi$  is closely analogous to the transformation in the Lieb-Schultz-Mattis [52] argument, and it was shown [53, 54] that a spin liquid state in  $d = 2$  acquires the momentum change

$$\Delta P_x^t = \frac{\pi}{a_x} \frac{L_y}{a_y} \left( \text{mod} \frac{2\pi}{a_x} \right) \quad (\text{A5})$$

where the second factor on the r.h.s. now counts the number of rows which have undergone the Lieb-Schultz-Mattis transformation. Now using  $\Delta P_x = \Delta P_x^q + \Delta P_x^t$ , we now obtain the modified Luttinger theorem obeyed in the FL\* phase:

$$2 \frac{v_0}{(2\pi)^2} \mathcal{V}_{FL^*} = (\rho_a - 1) \pmod{2}. \quad (\text{A6})$$

It is clear that the above argument is easily extended to a  $Z_2$  FL\* state in  $d = 3$ . The case of  $U(1)$  FL\* state in  $d = 3$  is somewhat more delicate because there is now a gapless spectrum of gauge fluctuations which can contribute to the evolution of the wavefunction under the flux insertion; nevertheless, the momentum change in (A5) corresponds to an allowed gauge flux, and we expect that (A5) continues to apply.



## APPENDIX B: TOY MODEL WITH U(1) FRACTIONALIZATION AND A SPINON FERMION SURFACE

In this Appendix, we will display a concrete model in three spatial dimensions that is in a U(1) fractionalized phase in three dimensions, and has a Fermi surface of spinons coupled to a gapless U(1) gauge field. As discussed earlier, this spinon Fermi surface could eventually (at low energies) undergo various instabilities including in particular to a spin density wave state.

Consider the following model:

$$\begin{aligned}
 H &= H_{t\psi} + H_{\Delta} + H_b + H_u + H_U, \\
 H_{t\psi} &= - \sum_{\langle rr' \rangle} t (\psi_r^\dagger \psi_{r'} + \text{h.c.}), \\
 H_{\Delta} &= \Delta \sum_{\langle rr' \rangle} e^{i\phi_{rr'}} (\psi_{r\uparrow}^\dagger \psi_{r'\downarrow}^\dagger - \psi_{r'\uparrow}^\dagger \psi_{r\downarrow}^\dagger) + \text{h.c.}, \\
 H_b &= -w \sum_{[rr'r'']} \cos(\phi_{rr'} - \phi_{rr''}), \\
 H_u &= u \sum_{\langle rr' \rangle} n_{rr'}^2, \\
 H_U &= U \sum_r (N_r - 1)^2.
 \end{aligned} \tag{B1}$$

Here  $\psi_r$  destroys a spinful charge-1 electron at each site of a cubic lattice in three spatial dimensions;  $e^{i\phi_{rr'}}$  creates a charge-2, spin-0 “Cooper pair” that resides on the links.  $n_{rr'}$  is conjugate to  $\phi_{rr'}$  and may be regarded as the Cooper pair number associated with each link.  $N_r$  is the total charge associated with each site and is given by

$$N_r = \sum_{r' \in r} n_{rr'} + \psi_r^\dagger \psi_r. \tag{B2}$$

The Hamiltonian  $H$  may be regarded as describing a system of electrons coupled with strong phase fluctuations. The first term in  $H_b$  represents Josephson coupling between two “nearest neighbor” bonds.  $H_u$  penalizes fluctuations in the Cooper pair number at each bond.  $H_U$  penalizes fluctuations in the total charge  $N_r$  that can be associated with each lattice site. The total charge of the full system clearly is

$$N_{\text{tot}} = \sum_r N_r. \tag{B3}$$

Depending on the various model parameters, several distinct phases are possible. Here we focus on the limit of large  $U$ . Diagonalizing  $H_U$  requires that the ground state(s) satisfy  $N_r = 1$  at all sites  $r$ . There is a gap of order  $U$  to states that do not satisfy this condition. Clearly the system is insulating in this limit.

The condition  $N_r = 1$  for all  $r$  still allows for a huge degeneracy of ground states which will be split once the other terms in the Hamiltonian are included. This splitting may be described by deriving an effective Hamiltonian that lives in the space of degenerate states specified

by  $N_r = 1$ . As discussed in Ref. 14, this effective Hamiltonian may be usefully viewed as a (compact) U(1) gauge theory. This may be explicitly brought out in the present case by the change of variables

$$\begin{aligned}
 \phi_{rr'} &= \epsilon_r a_{rr'}, \\
 n_{rr'} &= \epsilon_r E_{rr'}
 \end{aligned} \tag{B4}$$

$$\begin{aligned}
 \psi_{r\alpha} &= f_{r\alpha} \text{ for } r \in A, \\
 \psi_{r\alpha} &= i\sigma_{\alpha\beta}^y f_{r\beta}^\dagger \text{ for } r \in B.
 \end{aligned} \tag{B5}$$

Here  $\epsilon_r = +1$  on the  $A$  sublattice and  $-1$  on the  $B$  sublattice. In terms of these variables, the constraint  $N_r = 1$  reads

$$\vec{\nabla} \cdot \vec{E} + f_r^\dagger f_r = 1 \tag{B6}$$

at each site  $r$ . (We note that both  $\vec{a}$  and  $\vec{E}$  may be regarded as vector fields defined on the lattice). At order  $w^2/U, u, t, \Delta$ , the effective Hamiltonian takes the form

$$\begin{aligned}
 H_{\text{eff}} &= H_K + H_u + H_f, \\
 H_K &= -K \sum_P \cos(\vec{\nabla} \times \vec{a}), \\
 H_u &= +u \sum_r \vec{E}^2, \\
 H_f &= -\Delta \sum_{\langle rr' \rangle} (e^{ia_{rr'}} f_r^\dagger f_{r'} + \text{h.c.}).
 \end{aligned} \tag{B7}$$

Here  $K = 2w^2/U$ , and the sum  $\sum_P$  runs over elementary plaquettes.  $H_{\text{eff}}$  together with the constraint may be viewed as a Hamiltonian for a compact U(1) gauge theory coupled to a gauge charge-1 fermionic matter field  $f$ . (Note that to leading order the  $t$  term does not contribute).  $H_{\text{eff}}$  still admits several different phases depending on its parameters. Of interest to us is the limit  $K \sim w^2/U \gg u$ . In this limit, monopoles of the compact U(1) gauge field will be gapped. Consequently at low energies, we may take the gauge field to be non-compact. The  $\cos(\vec{\nabla} \times \vec{a})$  term can then be expanded to quadratic order to get the usual Maxwell dynamics for the gauge field. The  $f$ -particles form a Fermi surface which is coupled to this gapless U(1) gauge field. Note that in the low-energy manifold with  $N_r = 1$  at all  $r$ , all excitations have zero physical electric charge. Thus the  $f$  particles are neutral fermionic spinons.

As with any Fermi surface, this spinon Fermi surface state could at low energies further undergo various instabilities to other states (density waves, pairing, etc) depending on the residual interactions between the spinons. There are various sources of such interactions: First there is the gauge interaction that is explicit in  $H_{\text{eff}}$  in the leading order. Then the  $t$  term contributes to  $H_{\text{eff}}$  at second order and leads to a quartic spinon-spinon interaction as well. The specific low-energy instability of the spinon Fermi surface will be determined by the details of the competition between these various sources of interaction, and will not be discussed further here for this model.

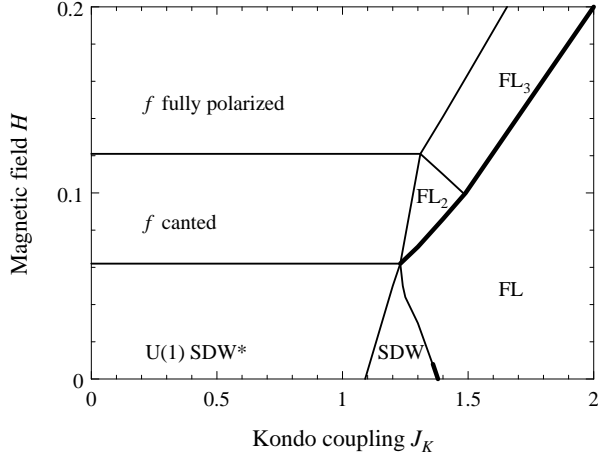


FIG. 8: Mean-field phase diagram of  $H_{\text{mf}}$  (18) on the cubic lattice, now as function of Kondo coupling  $J_K$  and external field  $H_z$  at  $T = 0$ . Parameter values are as in Fig. 4. For a description of the phases see text.

Apart from the deconfined phase discussed above, the model possesses confined phases; for large  $U$  those occur for smaller  $u$ , and the deconfinement transition occurs through the condensation of monopoles in the gauge field.

### APPENDIX C: MEAN-FIELD PHASE DIAGRAM IN AN EXTERNAL ZEEMAN MAGNETIC FIELD

In this Appendix we briefly discuss the behavior of the mean-field theory of Sec. IV C in an externally applied field. A sample zero-temperature phase diagram is displayed in Fig. 8, which shows very rich behavior.

The phases at small fields are straightforward generalizations of the low-temperature zero-field phases of Fig. 4: The U(1) SDW\* has weakly polarized conduction electrons,  $b_0 = 0$ , non-zero  $\chi_0$  indicating spinon hopping, and a canted spinon magnetization  $\vec{M}_r$  with a staggered component along  $\hat{x}$  and a uniform component along  $\hat{z}$ . The SDW phase has similar characteristics, but now  $b_0 \neq 0$  indicating a conventional weakly field-polarized magnet with confinement. Finally, the FL phase has  $b_0 \neq 0$ ,  $\chi_0 \neq 0$ , weakly polarized heavy quasiparticles, and the mean-field parameter  $\vec{M}_r$  has only a uniform  $z$  component.

In the small- $J_K$  region, increasing external field progressively suppresses the effect of  $H_H$ . At intermediate field, a phase with “canted”  $f$  moments arises, where now  $\chi_0 = b_0 = 0$  (no spinon hopping), and  $\vec{M}_r$  is canted as described above. Larger fields fully polarize the local moments, i.e.,  $\vec{M}_r$  points uniformly along  $\hat{z}$  with maximum amplitude, and  $\chi_0 = b_0 = 0$ . This phase is also realized for larger  $J_K$  and large fields – here the field quenches the Kondo effect. On the Fermi-liquid side of the phase diagram, two more phases arise in the present mean-field

theory which are labelled by FL<sub>2</sub> and FL<sub>3</sub> in Fig. 8; both have non-zero  $b_0$  and  $\chi_0$ . In FL<sub>2</sub>, the mean-field parameter  $\vec{M}_r$  has both staggered and uniform components, i.e., this phase describes canted, weakly screened local moments. Turning to the FL<sub>3</sub> phase, this high-field phase has the same symmetry characteristics as FL at intermediate fields, but a different Fermi surface topology. Whereas FL phase at intermediate fields has a single Fermi surface sheet for one spin direction (the majority spin have one full and one empty band whereas the minority spins have one partially filled and one empty band), in FL<sub>3</sub> the upper band of the majority spins becomes partially filled, too. FL and FL<sub>3</sub> are separated by a strongly first-order transition in mean-field theory. There are numerous other phase transitions associated with a change in the Fermi surface topology – those do not display strong thermodynamic signatures and are not shown. We note that for the field range displayed in Fig. 8,  $|\vec{H}_{\text{ext}}| \ll t$ , the conduction electrons are in general weakly affected by the field; significant polarization of them occurs only at much higher fields.

Notably, smaller values of the decoupling parameter  $x$  admit yet another field-induced transition in the small- $J_K$  region: If the magnetism is very weak, i.e., the spinons have a small gap compared to their bandwidth, then a small applied field can close the spinon gap without significantly affecting their band structure. Such a transition would yield a kink in the magnetization of the local-moment subsystem as function of the applied field, implying a “metamagnetic” behavior which is here generically associated with a *continuous* transition.

### APPENDIX D: SPECIFIC HEAT SINGULARITY

Here we present some details on the calculation of the singular specific heat coming from gauge fluctuations. The calculations in the FL\* phase and at the critical point are standard. We will therefore only consider the FL phase. In this phase close to the critical point, transverse gauge fluctuations are described by the action

$$S = \int \frac{d^3k}{(2\pi)^3} \frac{1}{\beta} \sum_{\omega_n} \left( \frac{|\omega_n|}{k} + k^2 + \rho_s \right) |\vec{a}(\vec{k}, \omega_n)|^2. \quad (\text{D1})$$

As explained in Section V, close to the transition  $\rho_s \sim b_0^2$ . This gives a free energy

$$F = \frac{2}{\beta} \sum_{\omega_n} \int \frac{d^3k}{(2\pi)^3} \ln \left( \frac{|\omega_n|}{k} + k^2 + \rho_s \right). \quad (\text{D2})$$

To calculate the low-temperature specific heat, we need the change in free energy on going from zero to a small non-zero temperature. After a Poisson resummation this is given by

$$\delta F(T) \equiv F(T) - F(0) \quad (\text{D3})$$

$$\begin{aligned}
&= 2 \int_{\vec{k}} \sum_{m \neq 0} \int \frac{d\omega}{2\pi} e^{i\beta m\omega} \ln \left( \frac{|\omega|}{k} + k^2 + \rho_s \right) \\
&= 2 \int_{\vec{k}, \omega} \int_0^\infty d\lambda \sum_{m \neq 0} \frac{k e^{i\beta m\omega}}{|\omega| + k(k^2 + \rho_s + \lambda)} \\
&= 2 \int_{\vec{k}, \omega, \lambda} \sum_{m \neq 0} k \int_0^\infty du e^{i\beta m\omega - u(|\omega| + k(k^2 + \rho_s + \lambda))}.
\end{aligned}$$

The  $\omega, \lambda$  integrals may now be performed to obtain

$$\begin{aligned}
\delta F(T) &= \frac{4}{\pi} \int_{\vec{k}} \sum_{m=1}^\infty \int du \frac{e^{-uk(k^2 + \rho_s)}}{u^2 + (m\beta)^2} \\
&= \int_0^\Lambda \frac{dk k^2}{2\pi^3} \int_u^\infty \frac{(\pi u T \coth(\pi u T) - 1) e^{-uk(k^2 + \rho_s)}}{u^2}.
\end{aligned}$$

In the last equation we have introduced an upper cut-off  $\Lambda$  for the momentum integral. The remaining integrals can now be straightforwardly evaluated for small  $T$ , and we find

$$\delta F(T) = \frac{T^2}{12\pi} \ln \left( \frac{\Lambda^2}{\rho_s} \right). \quad (D4)$$

Thus the specific heat

$$C(T) = \gamma T \quad (D5)$$

with  $\gamma \sim \ln(1/\rho_s) \sim \ln(1/b_0)$ . Setting  $\rho_s = 0$ , a similar calculation also shows that  $C(T) \sim T \ln(1/T)$  in the FL\* phase.

For completeness, we mention the corresponding behavior in two dimensions. In analogy to the above calculations, we find  $C(T) \propto T^{2/3}$  in the quantum-critical and FL\* regions.

## APPENDIX E: DETAILS OF THE QUANTUM BOLTZMANN EQUATION

In the following we describe a few details of the derivation of the linearized version of the quantum Boltzmann

equation (42) in Sec. V C. Inserting the ansatz (38) into Eq. (37) leads to a scalar equation for  $f_1$ . The frequency integral is easily performed; the remaining momentum integral can be split into radial and angular part. This directly yields Eq. (42), with

$$\begin{aligned}
K_1(\vec{k}, \vec{k}_1) &= [1 + f_0(\vec{k}) + n(\vec{k}^2 - \vec{k}_1^2)] \\
&\times \frac{\vec{k} \vec{k}_1^2}{4\pi^2} \int_{-1}^1 dx K \left( x, \frac{\vec{k}_1}{k}, \vec{k} \sqrt{T} \right), \quad (E1)
\end{aligned}$$

$$\begin{aligned}
K_2(\vec{k}, \vec{k}_1) &= [f_0(\vec{k}) - n(\vec{k}^2 - \vec{k}_1^2)] \\
&\times \frac{\vec{k} \vec{k}_1^2}{4\pi^2} \int_{-1}^1 dx \frac{x \vec{k}_1}{k} K \left( x, \frac{\vec{k}_1}{k}, \vec{k} \sqrt{T} \right) \quad (E2)
\end{aligned}$$

with  $f_0(x) = [\exp(x^2 + \bar{u}\sqrt{T}) - 1]^{-1}$  and  $n(x) = (e^x - 1)^{-1}$ . The kernel  $K(x, \vec{k}_1/k, \vec{k}\sqrt{T})$  is given by

$$\begin{aligned}
K(x, \alpha, \lambda) &= \text{Im} \left( -i \frac{1 - \alpha^2}{\sqrt{\alpha^2 + 1 - 2\alpha x}} + \lambda(\alpha^2 + 1 - 2\alpha x) \right)^{-1} \\
&\times \left( 1 - \frac{(\alpha x - 1)^2}{\alpha^2 + 1 - 2\alpha x} \right).
\end{aligned}$$

The integrals necessary for the evaluation of  $K_{1,2}$  are of the form

$$\int dy \frac{y^{n-1/2}}{y^3 + C}$$

with  $n = 0, \dots, 3$  and can be performed analytically.

The numerical solution of Eq. (42) is done by re-writing it in the form

$$\begin{aligned}
\psi(\vec{k}) &= -f'_0(\vec{k}) \\
&\times \left( \int_0^\infty d\vec{k}_1 \left[ K_1(\vec{k}, \vec{k}_1) + K_2(\vec{k}, \vec{k}_1) \frac{\psi(\vec{k}_1)}{\psi(\vec{k})} \right] \right)^{-1}
\end{aligned}$$

which allows for a stable numerical iteration.

- 
- [1] S. Doniach, *Physica B* **91**, 231 (1977).
  - [2] P. Coleman, C. Pépin, Q. Si, and R. Ramazashvili, *J. Phys: Condens. Matter* **13**, 723 (2001).
  - [3] G. R. Stewart, *Rev. Mod. Phys.* **73**, 797 (2001).
  - [4] H. v. Löhneysen, *J. Phys. Cond. Matter* **8**, 9689 (1996).
  - [5] A. Schröder, G. Aeppli, R. Coldea, M. Adams, O. Stockert, H. v. Löhneysen, E. Bucher, R. Ramazashvili, and P. Coleman, *Nature* **407**, 351 (2000).
  - [6] M. T. Béal-Monod and K. Maki, *Phys. Rev. Lett.* **34**, 1461 (1975).
  - [7] J. A. Hertz, *Phys. Rev. B* **14**, 1165 (1976).
  - [8] T. Moriya, *Spin Fluctuations in Itinerant Electron Magnetism*, Springer-Verlag, Berlin (1985); T. Moriya and T. Takimoto, *J. Phys. Soc. Jpn.* **64**, 960 (1995).
  - [9] G. G. Lonzarich and L. Taillefer, *J. Phys. C* **18**, 4339 (1985); G. G. Lonzarich, in *Electron*, M. Springford ed., Cambridge University Press, Cambridge (1997).
  - [10] A. J. Millis, *Phys. Rev. B*, **48**, 7183 (1993).
  - [11] T. Senthil, S. Sachdev, and M. Vojta, *Phys. Rev. Lett.* **90**, 216403 (2003).
  - [12] N. Read and S. Sachdev, *Phys. Rev. Lett.* **66**, 1773 (1991); X.-G. Wen, *Phys. Rev. B* **44**, 2664 (1991).
  - [13] T. Senthil and M. P. A. Fisher, *Phys. Rev. B* **62**, 7850 (2000); *Phys. Rev. B* **63**, 134521 (2001).
  - [14] O. I. Motrunich and T. Senthil, *Phys. Rev. Lett.* **89**, 277004 (2002); X.-G. Wen, *Phys. Rev. B* **68**, 115413 (1993).

- (2003).
- [15] L. Balents, M. P. A. Fisher and C. Nayak, Phys. Rev. B **60**, 1654 (1999).
  - [16] A. C. Hewson, *The Kondo Problem to Heavy Fermions*, Cambridge University Press, Cambridge, 1993.
  - [17] D. M. Newns and N. Read, Adv. in Phys. **36**, 799 (1987).
  - [18] P. Coleman, Phys. Rev. B **35**, 5072 (1987).
  - [19] P. B. Weichman, M. Rasolt, M. E. Fisher, and M. J. Stephen, Phys. Rev. B **33**, 4632 (1986).
  - [20] Chapter 11 of S. Sachdev, *Quantum Phase Transitions*, Cambridge University Press, Cambridge, 1999.
  - [21] The absence of a phase transition in three spacetime dimensions for the theory of a complex scalar coupled to a compact U(1) gauge field was noted *e.g.* in N. Nagaosa and P. A. Lee, Phys. Rev. B **61**, 9166 (2000). The theory of a complex scalar coupled to a non-compact U(1) gauge field is well known to be dual to the XY model (C. Dasgupta and B. I. Halperin, Phys. Rev. Lett. **47**, 1556 (1981)), with the dual XY field representing a vortex operator. Under the same duality transformation, the compact theory maps onto the XY model in a “magnetic” field, with the “magnetic” field allowing for monopoles at which vortex lines can terminate. The XY model in a field is not expected to have any phase transition.
  - [22] L. B. Ioffe and G. Kotliar, Phys. Rev. B **42**, 10348 (1990).
  - [23] P. A. Lee and N. Nagaosa, Phys. Rev. B **46**, 5621 (1992).
  - [24] N. Andrei and P. Coleman, Phys. Rev. Lett. **62**, 595 (1989).
  - [25] Yu. Kagan, K. A. Kikoin, and N. V. Prokof'ev, Physica B **182**, 201 (1992).
  - [26] S. Burdin, D. R. Grempel, and A. Georges, Phys. Rev. B **66**, 045111 (2002).
  - [27] E. Demler, C. Nayak, H.-Y. Kee, Y.-B. Kim, and T. Senthil, Phys. Rev. B **65**, 155103 (2002).
  - [28] F. H. L. Essler and A. M. Tsvelik, Phys. Rev. B **65**, 115117 (2002).
  - [29] In our paper, we are using the term “Luttinger’s theorem” to simply be equivalent to the statement that the volume enclosed by the Fermi surface counts all electrons. With this definition, the state proposed by Essler and Tsvelik [28] does amount to a violation of “Luttinger’s theorem”. However, in their case, the violation of the formal many body proof of Oshikawa can be understood in the context of renormalized perturbation theory. In our models, the violation is intimately linked to topological order, and cannot be understood by any perturbative analysis of the electron Hamiltonian.
  - [30] Q. Si, S. Rabello, K. Ingersent, and J. L. Smith, Nature **413**, 804 (2001) and Phys. Rev. B **68**, 115103 (2003).
  - [31] P. Sun and G. Kotliar, Phys. Rev. Lett. **91**, 037209 (2003).
  - [32] J.-X. Zhu, D. R. Grempel, and Q. Si, cond-mat/0304033.
  - [33] M. Hermele, L. Balents, M.P.A. Fisher, cond-mat/0305401.
  - [34] Quite generally a U(1) deconfined state necessarily requires a conserved U(1) gauge charge for the spinons. In contrast, in a state described by a deconfined  $Z_2$  gauge theory, consistency only requires a conserved  $Z_2$  charge for the spinons: this implies that the spinons will generically be paired in  $Z_2$  states but not in the U(1) states.
  - [35] In particular, the monopole gap will survive a weak Kondo coupling.
  - [36] N. Read, D. M. Newns, and S. Doniach, Phys. Rev. B **30**, 3841 (1984).
  - [37] A. J. Millis and P. A. Lee, Phys. Rev. B **35**, 3394 (1987).
  - [38] T. Holstein, R. Norton, and P. Pincus, Phys. Rev. B **8**, 2649 (1973); M. Yu. Reizer Phys. Rev. B **40**, 11571 (1989).
  - [39] Depending on the model parameters, a number of mean-field phases in which the  $\chi$  fields break translational symmetry are possible. In particular, the FL\* and SDW\* states of Sec. IV C are unstable to dimerization; note that in three dimensions this instability is weaker than the corresponding one in  $d = 2$ . For the square lattice, it has been found that ring exchange stabilizes spatially homogeneous mean-field solutions (O. I. Motrunich, private communication), therefore we expect that the inclusion of ring exchange can yield stable spin-liquid saddle points in  $d = 3$  as well.
  - [40] E. Fradkin and S. Shenker, Phys. Rev. D **19**, 3682 (1979).
  - [41] M. P. A. Fisher, P. B. Weichmann, G. Grinstein, and D. S. Fisher, Phys. Rev. B **40**, 546 (1989).
  - [42] The fate of the monopoles at this transition is analogous to the fate of gapped spinons on going from a spin liquid to a spin-Peierls state: though the spin gap does not close, the spinons exist only on one side of the transition and play no role in the universal low-energy critical properties.
  - [43] L. Ioffe and A. Larkin, Phys. Rev. B **39**, 8988 (1989).
  - [44] Y.-B. Kim, P. A. Lee, and X.-G. Wen, Phys. Rev. B **52**, 17275 (1995).
  - [45] K. Damle and S. Sachdev, Phys. Rev. B **56**, 8714 (1997).
  - [46] N. Nagaosa and P. A. Lee, Phys. Rev. B **43**, 1233 (1991).
  - [47] B. L. Altshuler, L. B. Ioffe, and A. J. Millis, Phys. Rev. B **50**, 14048 (1994); B. L. Altshuler, L. B. Ioffe, A. I. Larkin, and A. J. Millis, Phys. Rev. B **52**, 4607 (1995).
  - [48] Rosch *et al.* [Phys. Rev. Lett. **79**, 159 (1997)] considered two-dimensional spin fluctuations coupled to three-dimensional electrons to explain the  $T \ln T$  behavior of the specific heat in  $\text{CeCu}_{6-x}\text{Au}_x$ ; this theory cannot easily account for the neutron scattering results of Ref. [5]. Si *et al.* [30] proposed an extended dynamical mean-field theory which, in  $d = 2$ , aims on modelling the results of Ref. [5]. In  $d = 3$ , this theory leads to a conventional SDW transition of a Fermi liquid.
  - [49] P. Gegenwart, J. Custers, C. Geibel, K. Neumaier, T. Tayama, K. Tenya, O. Trovarelli, and F. Steglich, Phys. Rev. Lett. **89**, 056402 (2002).
  - [50] See, *e.g.*, S. Sachdev and K. Park, Annals of Physics, N.Y. **298**, 58 (2002).
  - [51] M. Oshikawa, Phys. Rev. Lett. **84**, 3370 (2000).
  - [52] E. H. Lieb, T. Schultz, and D. J. Mattis, Ann. Phys. (N.Y.) **16**, 407 (1961).
  - [53] N. E. Bonesteel, Phys. Rev. B **40**, 8954 (1989).
  - [54] G. Misguich, C. Lhuillier, M. Mambrini, and P. Sindzinger, Eur. Phys. J. B **26**, 167 (2002).